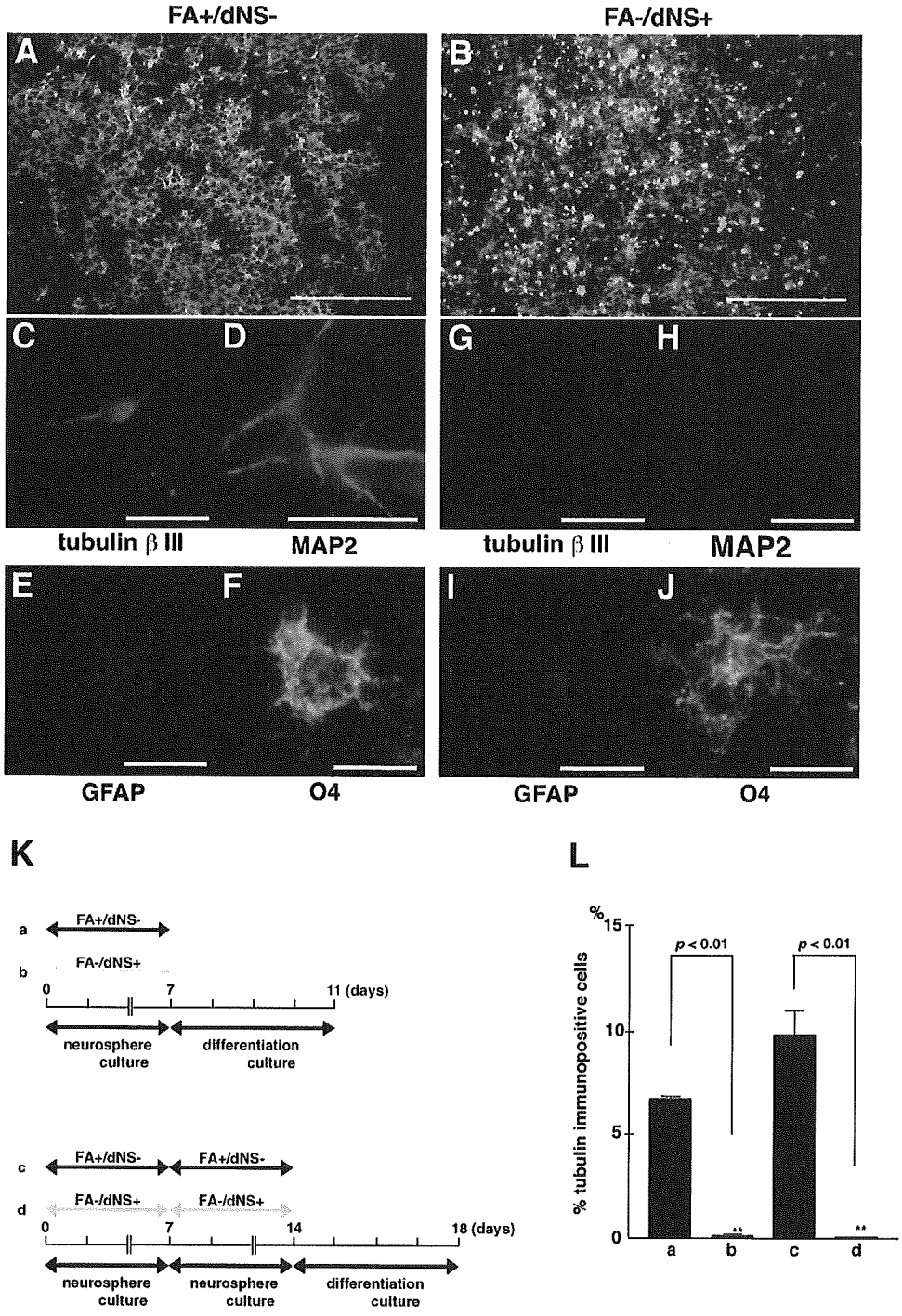

Fig. 5 – Tri-colored immunofluorescence of markers for neurons (tubulin β III, red), astrocytes (GFAP, blue), and oligodendrocytes (O4, *green*) shows that the FA+/dNS– clonal spheres gave rise to different cells expressing markers of all three neural cell types, as depicted in a triple-labeled survey (A), and the details of individual cells of each type (C–F). The FA–/dNS+ spheres gave rise to astrocytes and oligodendrocytes, but not neurons, as shown in a triple-labeled survey (B), which also depicted the details of individual cells (G–J). Scale bars: A, B, 200 μm; C–J, 20 μm. (K) Experimental protocol. The 7-DIV primary culture in the FA–/dNS+ (a) and FA+/dNS– (b) condition was placed under the differentiation condition for 4 DIV (total 11 DIV). (c), The 7-DIV primary culture in the FA+/dNS– medium was placed under the FA+/dNS– condition for 7 DIV (total 14 DIV) and, then, the cultured cells were placed under the differentiation condition for 4 DIV (total 18 DIV). (d) Likewise, the FA–/dNS+ primary culture was placed under the FA–/dNS+ condition and, then, under the differentiation condition. (L) Graph showing mean ± SEM percentage of tubulin β III-immunopositive neurons of the total number of cells per field derived from each protocol. **Significant difference between the two groups ($P < 0.01$).

2.5. *In vitro differentiation analysis of sphere-initiating cells in the FA+/dNS− or FA−/dNS+ media*

To examine the multipotency of spheres under the FA+/dNS− and FA−/dNS+ conditions, we transferred and placed isolated spheres under the differentiation condition. After 4 DIV of differentiation, triple-labeled immunocytochemistry for tubulin β III, GFAP, and O4 revealed that cells with the morphological and antigenic characteristics of neurons, astrocytes, and oligodendrocytes, respectively, were generated from the FA+/dNS− spheres (Figs. 5A, C–F). In contrast, the FA−/dNS+ spheres yielded astrocytes and oligodendrocytes, but neither tubulin β III nor MAP2 positive neurons (Figs. 5B, G–I). The percentage of tubulin β III positive neurons that differentiated from the FA−/dNS+ primary spheres was 0.067% ± 0.009% (n = 4) significantly lower than that from the FA+/dNS− primary spheres (6.618% ± 0.188%, n = 5, $P < 0.01$), as well as the percentage of tubulin β III positive neurons from secondary spheres (FA−/dNS+, 0.035% ± 0.004% vs. FA+/dNS−, 9.81% ± 1.516%, n = 4, $P < 0.01$) (Fig. 5J). According to previous studies, the percentage of neurons derived from the neurosphere culture under the regular condition was 5%–10% (Laeng et al., 2004; Palmer et al., 1999). These results suggested that spheres formed under the FA+/dNS− condition, but not under the FA−/dNS+ condition, coincided with the definition of a neurosphere, self-renewal capability, and multipotency (Seaberg and van der Kooy, 2002).

2.6. *Effects of inhibitors of de novo DNA synthesis on in vitro differentiation*

We hypothesized that the disturbance of de novo DNA synthesis in the sphere-forming neural stem cells resulted in the decrease of neurons. To test the hypothesis, we added de novo synthesis inhibitors to the FA+/dNS+ medium. AZP blocks the conversion of inosinate to adenyl succinate, which is the key reaction in the formation of purine adenylate; additionally, it also blocks an important step in the production of the purine base guanylate (Belgi and Friedmann, 2002) (Fig. 1). MTX is a competitive inhibitor of dihydrofolate reductase (EC 1.5.1.3), which generates tetrahydrofolate from dihydrofolate. As a result, MTX interferes with the conversion of deoxyuridylate to thymidylate in the synthesis of DNA (Olsen, 1991) (Fig. 1). Both AZP and MTX inhibited sphere formation in a dose-dependent manner (Figs. 6A–C). The inhibition was most evident under the FA+/NS− condition. These results suggested that lower doses of AZP and MTX (e.g., <1 μM) selectively inhibited the de novo DNA synthesis in sphere-forming cells. We transferred the spheres obtained under these conditions and placed them under the differentiation condition (Fig. 6D). After 4 DIV, the percentage of tubulin β III positive neurons derived from the FA+/dNS+ spheres significantly (n = 4, $P < 0.01$) decreased in the presence of AZP or MTX (Fig. 6E). Figs. 6F–I show representative fields of the culture under the FA+/dNS+ condition (Fig. 6F), FA−/dNS+ condition (Fig. 6G), FA+/dNS+ with 1 μM AZP condition (Fig. 6H), and FA+/dNS+ with 0.1 μM MTX condition (Fig. 6I). The number of astrocytes did not significantly differ among these conditions (data not shown).

3. Discussion

We performed the neurosphere method by using modified media that lacked FA or dNS and added specific inhibitors of DNA synthesis. Cultured cells barely proliferated and underwent apoptosis under the FA−/dNS− condition. Although sphere formation was observed, the spheres formed under the FA−/dNS+ condition poorly produced neurons. Since extracellular nucleosides exert various effects on cell differentiation, apoptosis, mitogenesis, and stimulators of cytokine release in the nervous system (Neary et al., 1996), the decreased percentage of neurons derived from the FA−/dNS+ spheres could be attributed to the effects of extracellular nucleosides. However, there was no significant difference ($P > 0.05$) between the percentage of neurons derived from FA+/dNS+ spheres (7.662 ± 1.672%, n = 4) (Fig. 6E) and FA+/NS− spheres (6.618% ± 0.188%, n = 5) (Fig. 5J). Addition of inhibitors of de novo DNA synthesis, namely, AZP and MTX, resulted in poor neuronal differentiation even under the FA+/dNS+ condition. Taken together, low percentage of neurons derived from spheres formed under the FA−/dNS+ condition is not due to the extracellular effects of dNS, but due to the proliferation failure of sphere-forming neural stem cells induced by inactivation of the de novo DNA synthesis pathway.

The neurosphere cultures established from the E12.5 mouse proliferated to a lesser extent than those obtained from the E14.5 or E16.5 mouse under the FA−/dNS+ condition, while they proliferated to an equivalent extent under the FA+/dNS− condition. As shown in the differentiation assay, FA−/dNS+ spheres were likely to consist of cells committed to the glial lineage (Seaberg and van der Kooy, 2002). This result may be in line with the fact that neurogenesis precedes gliogenesis (Qian et al., 2000). To clarify the mechanism responsible for the developmental change in the DNA synthesis pathway, we compared the mRNA expression of thymidine kinase (EC. 2.7.1.21), deoxycytidine kinase (EC. 2.7.1.74), and adenosine kinase (EC. 2.7.1.45)—key enzymes for the salvage pathway (Karbownik et al., 2003)—and that of thymidylate synthetase (EC. 2.1.1.45)—a key enzyme for the de novo pathway (Chu et al., 2003)—in the E11.5 and E16.5 mouse neuroepithelium. There was no detectable change in semi-quantitative RT-PCR (data not shown). The activities of several key enzymes involved in DNA synthesis were previously reported using developmental brain tissues (Hyndman and Zamenhof, 1978; Suleiman and Spector, 1982; Sung, 1971). These reports suggested that the specific activities of both the DNA synthesis pathways equally decreased in proportion with maturation. Since there is a discrepancy between the mRNA levels and enzymatic activities, the activities of the key enzymes involved in the DNA synthesis pathways may also be regulated translationally and/or posttranslationally (Ayusawa et al., 1986; Sherley and Kelly, 1988).

FA is a cofactor in one-carbon metabolism, and it promotes the remethylation of homocysteine. Folate deficiency allows the accumulation of intracellular homocysteine, a potentially neurotoxic amino acid that can induce DNA strand break, thereby triggering apoptosis (Mattson

and Shea, 2003). FA deficiency and elevated homocysteine levels endanger postmitotic neurons in neurodegenerative disease model mice (Duan et al., 2002; Kruman et al., 2002). To test the effect of homocysteine on sphere-forming neural stem cells, we performed a neurosphere assay in the FA+/dNS+ medium supplemented with 0.1–1000 μM homocysteine. However, no toxic effect was observed with any concentration of homocysteine. Additionally, no inhibitory effect of homocysteine on neuronal differentiation was observed in the in vitro differentiation assay (unpublished data). These results suggest that the high concentration of homocysteine due to FA deficiency cannot explain the proliferation failure of neural stem cells observed in our study.

De novo DNA synthesis inhibitors, such as MTX and AZP, are reported to induce selective malformation of the rhombencephalic and telencephalic brain regions in rat embryo cultures (Schmid, 1984) and neural tube defects (NTD) in rabbits (Lloyd et al., 1999). In humans, NTD can be prevented by FA supplementation in the periconceptual period (Czeizel and Dudas, 1992; Daly et al., 1995). Although FA deficiency does not cause NTDs in normal mice (Heid et al., 1992) or in cultured rat embryos (Cockroft, 1991), Fleming and Copp (1998) identified a mouse model of NTD, namely, homozygous Splotch (Pax3) mouse embryos, in which exogenous FA and thymidine prevent NTDs in culture. This observation suggested that the disturbance of DNA synthesis was involved in the pathogenesis of NTDs.

Our observation may explain the vulnerability of embryonic brain to FA deficiency. Craciunescu et al. (2004) reported that FA deficiency decreased progenitor cell proliferation and increased apoptosis in the fetal mouse brain (Craciunescu et al., 2004). In this study, we showed that the activity of de novo DNA synthesis is necessary for primary cultured neural stem cells to proliferate with multipotency. Glial cells can proliferate under the activation of either de novo or salvage DNA synthesis pathway whereas neuronal cells cannot be generated under the activation of salvage pathway alone. Neural tube defect can be prevented by administration of FA during the periconceptual period, which may result from activation of de novo DNA synthesis and differentiation to neurons from neural stem cells. Further studies are necessary to elucidate a role of de novo DNA synthesis pathway in differentiation from neural stem cells into neurons in both embryonic and adult central nervous system.

4. Experimental procedures

4.1. *Neurosphere culture*

Neurosphere cultures were prepared as described previously (Reynolds and Weiss, 1996). In brief, striata were removed from E12.5, E14.5, and E16.5 C57BL/6 mice (Japan SLC, Hamamatsu, Japan) embryos and were mechanically dissociated. In place of the complete D-MEM/F-12 medium (Invitrogen, San Diego, CA), which contains 6 μM FA, 1.5 μM Thy, and 1.5 μM hypoxanthine, the cells were cultured in a custom-prepared deficient D-MEM/F-12 medium lacking FA, Thy, and hypoxanthine in order to stress the availability of precursors for both the de novo pathway (folate derivatives) and salvage pathway (Thy, hypoxanthine) of DNA synthesis. The cells were resuspended in the deficient D-MEM/F-12 medium supplemented with N-2 supplement (Invitrogen) (progesterone, 20 nM; apo-transferrine, 100 μM; sodium selenite, 30 nM; insulin, 25 μg/ml), 20 ng/ml human recombinant (hr–) basic FGF-2 (R&D Systems, Minneapolis, MN), 20 ng/ml hr-EGF (Upstate Biotechnology, Lake Placid, NY), and various concentrations of FA and dNS as described. FA was purchased from Takeda Pharmaceutical Co. Ltd. (Tokyo, Japan) and prepared as a 15 mg/ml stock solution before it was added to the culture at a final concentration of 1.0–400 μM. 2′-deoxyadenosine (dAdo), 2′-deoxycytidine (dCyd), 2′-deoxyguanosine (dGuo), Thy, azathioprine (AZP), and methotrexate (MTX) were purchased from Sigma (St. Louis, MO) and prepared as a 20 mM stock solution in water. Viable single cells at a density of 1.0×10^5 cells/ml were seeded into 75-cm^2 tissue culture flasks and incubated at 37 °C in an atmosphere of 5% CO_2 and treated with 20 ng/ml basic fibroblast growth factor (bFGF) every other day. Secondary neurosphere cultures were prepared by mechanical dissociation of 7 days in vitro (DIV) primary neurospheres into single cells and resuspended at a density of 2.0×10^4 cells/ml in a fresh culture medium. For neurosphere counting, viable single cells at a density of 1.0×10^4 cells/ml were seeded into uncoated 96-well microplates. It has been demonstrated previously that culturing cells at this density will result in clonal neurosphere colonies, as form in single-cell cultures, and that neurospheres do not arise as a result of cell aggregation at the cell culture densities used here (Seaberg and van der Kooy, 2002; Tropepe et al., 2000). To assess their differentiation potential, 7-DIV spheres were plated onto poly-L-ornithine-coated chamber slides (Nunc, Naperville, IL) in D-MEM/F-12 supplemented with N-2 supplement and 10% fetal bovine serum (differentiation condition) and cultured for 4 DIV before fixation for immunocytochemistry. For neuron counting, 7 DIV spheres were mechanically dissociated, and viable cells were resuspended at a density of 5.0×10^4 cells/ml and plated onto the precoated chamber slides under the differentiation condition. Cell numbers and viability were assessed by trypan blue dye exclusion by using a hemocytometer.

Fig. 6 – Inhibitors of de novo DNA synthesis decrease tubulin β III-immunopositive neurons in the neurosphere culture. (A) Experimental protocol. Neurospheres were cultured under the FA+/dNS–, FA–/dNS+, and FA+/dNS+ conditions supplemented with AZP or MTX for 7 DIV. (B and C) Dose–response curves of sphere formation, cultured for 7 DIV under each condition supplemented with AZP (B) and MTX (C). Among the three conditions, the FA+/dNS– condition was the most sensitive to the inhibitors. Graphs show mean ± SEM number of spheres per 1×10^4 cells. (D) Experimental protocol. Spheres formed under the conditions, as described above, were placed under the common differentiation condition. (E) Quantitative analysis of the effects of de novo inhibitors. Graph shows mean ± SEM percentage of tubulin β III-immunopositive neurons of the total number of cells per field derived from the spheres under the FA+/dNS+ condition or under the FA+/dNS+ condition with inhibitors. **Significant difference compared with the FA+/dNS+ condition ($P < 0.01$). (F–I) Double immunocytochemistry for neurons (tubulin β III, red) and astrocytes (GFAP, green). Representative fields derived from the spheres under the FA+/dNS+ conditions (F), FA–/dNS+ (G), FA+/dNS+ with 1 μM AZP (H), and FA+/dNS+ with 0.1 μM MTX (I) conditions are shown. White arrowheads indicate tubulin β III-positive neurons. Scar bars: F–I, 50 μM.

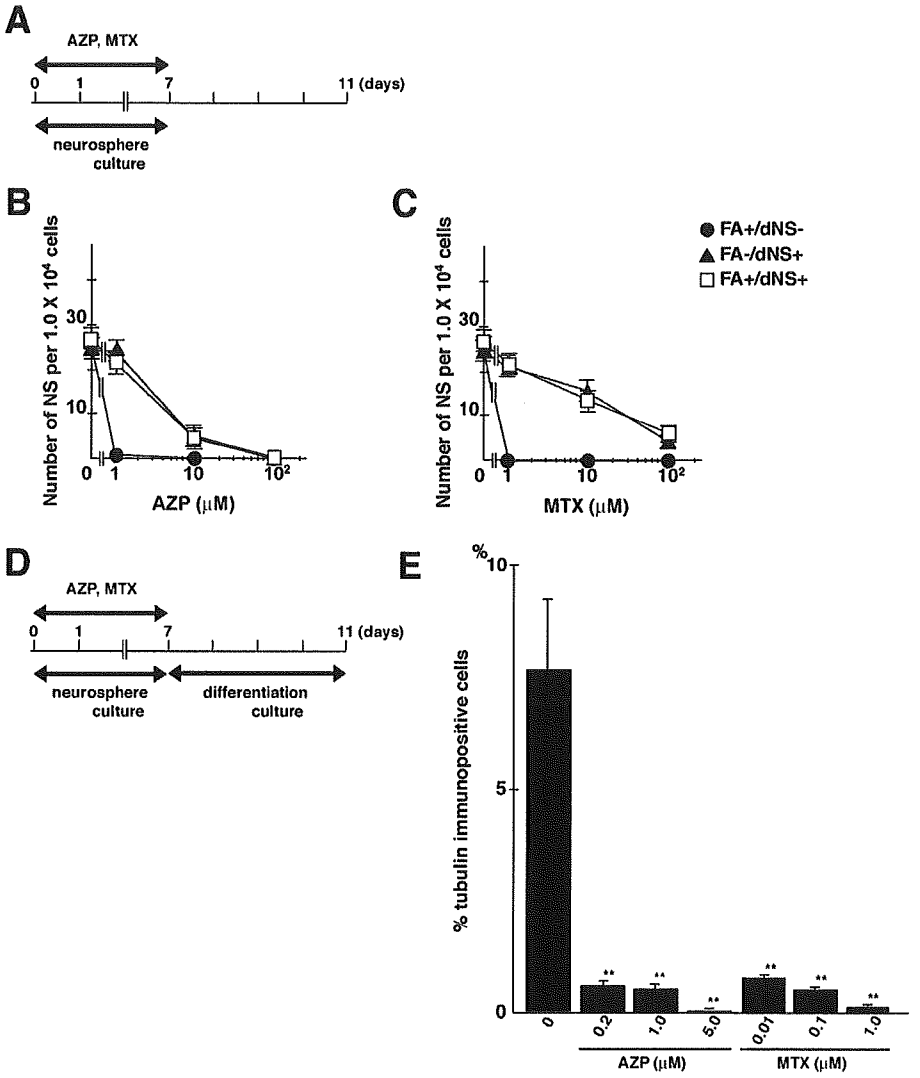
A
AZP, MTX
0
1
7
11 (days)
neurosphere culture
B
Number of NS per 1.0 X 10⁴ cells
30
10
0
1
10
10²
AZP (μM)
C
FA+/dNS-
FA-/dNS+
FA+/dNS+
Number of NS per 1.0 X 10⁴ cells
MTX (μM)
D
AZP, MTX
11 (days)
neurosphere culture
differentiation culture
E
% tubulin immunopositive cells
0
5
10
0.2
1.0
5.0
0.01
0.1
1.0
AZP (μM)
MTX (μM)

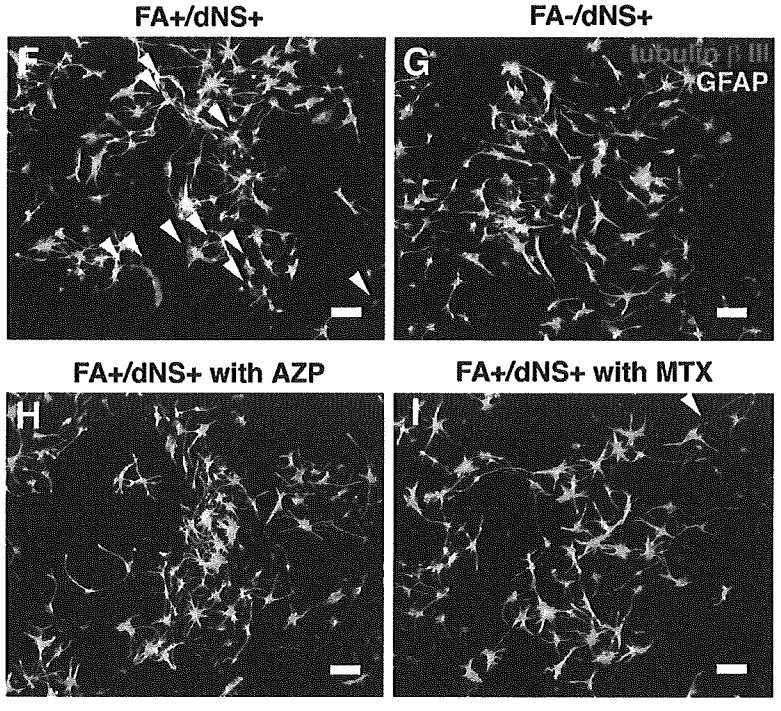
FA+/dNS+
FA-/dNS+
F
G
tubulin β III
GFAP
FA+/dNS+ with AZP
FA+/dNS+ with MTX
H
I

4.2. *Immunocytochemistry*

Indirect immunocytochemistry was carried out either immediately after plating (for neurosphere staining) or after 4 DIV (for triple-labeling and for neuronal counting). The cells plated on the precoated chamber slides were fixed in 4% paraformaldehyde for 30 min, followed by permeabilization with 0.3% Triton X-100 for 5 min, and stained by immunofluorescence with the following primary antibodies: mouse anti-tubulin β III (1:200; Chemicon, Temecula, CA), mouse anti-MAP2 (1:500; Chemicon), mouse anti-nestin (1:200; Chemicon), rabbit anti-GFAP (1:400; Dako, Carpinteria, CA), and mouse anti-O4 (1:20, Chemicon). Primary antibodies were visualized with Cy3- (red), AMCA- (blue), and FITC- (green) conjugated secondary antibodies (Jackson Immuno-Research, West Grove, PA). 4′,6-Diamidino-2-phenylindole (DAPI) was used as a fluorescent nuclear counterstain. Stained cultures were examined and photographed by fluorescence microscopy (Leica, Nussloch, Germany).

4.3. *Statistical analysis*

Statistical analyses were carried out using ANOVA or Student's *t* test. A *P* value <0.05 was considered significant.

REFERENCES

Ayusawa, D., Shimizu, K., Koyama, H., Kaneda, S., Takeishi, K., Seno, T., 1986. Cell-cycle-directed regulation of thymidylate synthase messenger RNA in human diploid fibroblasts stimulated to proliferate. J. Mol. Biol. 190, 559–567.

Belgi, G., Friedmann, P.S., 2002. Traditional therapies: glucocorticoids, azathioprine, methotrexate, hydroxyurea. Clin. Exp. Dermatol. 27, 546–554.

Chiasson, B.J., Tropepe, V., Morshead, C.M., van der Kooy, D., 1999. Adult mammalian forebrain ependymal and subependymal cells demonstrate proliferative potential, but only subependymal cells have neural stem cell characteristics. J. Neurosci. 19, 4462–4471.

Chu, E., Callender, M.A., Farrell, M.P., Schmitz, J.C., 2003. Thymidylate synthase inhibitors as anticancer agents: form bench to bedside. Cancer Chemother. Pharmacol. 52, S80–S89.

Cockroft, D.L., 1991. Vitamin deficiencies and neural-tube defects: human and animal studies. Hum. Reprod. 6, 148–157.

Craciunescu, C.N., Brown, E.C., Mar, M.H., Albright, C.D., Nadeau, M.R., Zeisel, S.H., 2004. Folic acid deficiency during late gestation decreases progenitor cell proliferation and increases apoptosis in fetal mouse brain. J. Nutr. 134, 162–166.

Czeizel, A.E., Dudas, I., 1992. Prevention of the first occurrence of neural-tube defects by periconceptional vitamin supplementation. N. Engl. J. Med. 327, 1832–1835.

Daly, L.E., Kirke, P.N., Molloy, A., Weir, D.G., Scott, J.M., 1995. Folate levels and neural tube defects. Implications for prevention. J. Am. Med. Assoc. 27, 1698–1702.

Duan, W., Ladenheim, B., Cutler, R.G., Kruman, I.I., Cadet, J.L., Mattson, M.P., 2002. Dietary folate deficiency and elevated homocysteine levels endanger dopaminergic neurons in models of Parkinson's disease. J. Neurochem. 80, 101–110.

Fleming, A., Copp, A.J., 1998. Embryonic folate metabolism and mouse neural tube defects. Science 280, 2107–2109.

Hatse, S., De Clercq, E., Balzarini, J., 1999. Role of antimetabolites of purine and pyrimidine nucleotide metabolism in tumor cell differentiation. Biochem. Pharmacol. 58, 539–555.

Heid, M.K., Bills, N.D., Hinrichs, S.H., Clifford, A.J., 1992. Folate deficiency alone does not produce neural tube defects in mice. J. Nutr. 122, 888–894.

Hyndman, A.G., Zamenhof, S., 1978. Thymidine phosphorylase, thymidine kinase and thymidylate synthetase activities in cerebral hemispheres of developing chick embryos. J. Neurochem. 31, 577–580.

James, S.J., Basnakian, A.G., Miller, B.J., 1994. In vitro folate deficiency induces deoxynucleotide pool imbalance, apoptosis, and mutagenesis in Chinese hamster ovary cells. Cancer Res. 54, 5075–5080.

Karbownik, M., Brzezianska, E., Zasada, K., Lewinski, A., 2003. Expression of genes for certain enzymes of pyrimidine and purine salvage pathway in peripheral blood leukocytes collected from patients with Graves' or Hashimoto's disease. J. Cell. Biochem. 89, 550–555.

Koury, M.J., Horne, D.W., 1994. Apoptosis mediates thymidine prevents erythroblast destruction in folate deficiency anemia. Proc. Natl. Acad. Sci. U. S. A. 99, 4067–4071.

Koury, M.J., Price, J.O., Hicks, G.G., 2000. Apoptosis in megaloblastic anemia occurs during DNA synthesis by a p53-independent, nucleoside-reversible mechanism. Blood 96, 3249–3255.

Kruman, I.I., Kumaravel, T.S., Lohani, A., Pedersen, W.A., Cutler, R.G., Kruman, Y., Haughey, N., Lee, J., Evans, M., Mattson, M.P., 2002. Folic acid deficiency and homocysteine impair DNA repair in hippocampal neurons and sensitize them to amyloid toxicity in experimental models of Alzheimer's disease. J. Neurosci. 22, 1752–1762.

Laeng, P., Pitts, R.L., Lemire, A.L., Drabik, C.E., Weiner, A., Tang, H., Thyagarajan, R., Mallon, B.S., Altar, C.A., 2004. The mood stabilizer valproic acid stimulate GABA neurogenesis from rat forebrain stem cells. J. Neurochem. 91, 238–251.

Laywell, E.D., Rakic, P., Kukekov, V.G., Holland, E.C., Steindler, D.A., 2000. Identification of a multipotent astrocytic stem cell in the immature and adult mouse brain. Proc. Natl. Acad. Sci. U. S. A. 97, 13883–13888.

Lloyd, M.E., Carr, M., McElhatton, P., Hall, G.M., Hughes, R.A., 1999. The effects of methotrexate on pregnancy, fertility and lactation. QJM 92, 551–563.

Mattson, M.P., Shea, T.B., 2003. Folate and homocysteine metabolism in neural plasticity and neurodegenerative disorders. Trends Neurosci. 26, 137–146.

Murray, R.K., Granner, D.K. (Eds.), 1999. Harper's Biochemistry, 25th edition. Appleton and Lange.

Neary, J.T., Rathbone, M.P., Cattabeni, F., Abbracchio, M.P., Burnstock, G., 1996. Trophic actions of extracellular nucleotides and nucleosides on glial and neuronal cells. Trends Neurosci. 19, 13–18.

Olsen, E.A., 1991. The pharmacology of methotrexate. J. Am. Acad. Dermatol. 25, 306–318.

Palmer, T.D., Markakis, E.A., Willhoite, A.R., Safar, F., Gage, F.H., 1999. Fibroblast growth factor-2 activates a latent neurogenic program in neural stem cells from diverse regions of the adult CNS. J. Neurosci. 19, 8487–8497.

Qian, X., Shen, Q., Goderie, S.K., He, W., Capela, A., Davis, A.A., Temple, S., 2000. Timing of CNS cell generation: a programmed sequence of neuron and glial cell production from isolated murine cortical stem cells. Neuron 28, 69–80.

Reynolds, B.A., Weiss, S., 1996. Clonal and population analyses demonstrate that an EGF-responsive mammalian embryonic CNS precursor is a stem cell. Dev. Biol. 175, 1–13.

Schmid, B.P., 1984. Monitoring of organ formation in rat embryos after in vitro exposure to azathioprine, mercaptopurine, methotrexate or cyclosporin A. Toxicology 31, 9–21.

Seaberg, R.M., van der Kooy, D., 2002. Adult rodent neurogenic regions: the ventricular subependyma contains neural stem cells, but the dentate gyrus contains restricted progenitors. J. Neurosci. 22, 1784–1793.

Sherley, J.L., Kelly, T.J., 1988. Regulation of human thymidine kinase during the cell cycle. J. Biol. Chem. 263, 8350–8358.

Sommer, L., Rao, M., 2002. Neural stem cells and regulation of cell number. Prog. Neurobiol. 66, 1–18.
Suleiman, S.A., Spector, R., 1982. Identification, development, and regional distribution of thymidylate synthetase in adult rabbit brain. J. Neurochem. 38, 392–396.
Sung, S.C., 1971. Thymidine kinase in the developing rat brain. Brain Res. 35, 268–271.
Tropepe, V., Coles, B.L.K., Chiasson, B.J., Horsford, D.J., Elia, A.J., McInnes, R.R., van der Kooy, D., 2000. Retinal stem cells in the adult mammalian eye. Science 287, 2032–2036.

HUMAN MUTATION 27(4), 343–352, 2006

RESEARCH ARTICLE

Comprehensive Mutation Analysis of *GLDC*, *AMT*, and *GCSH* in Nonketotic Hyperglycinemia

Shigeo Kure,[1]* Kumi Kato,[1,10] Agirios Dinopoulos,[2] Chuck Gail,[2] Ton J. deGrauw,[2] John Christodoulou,[3] Vladimir Bzduch,[4] Rozalia Kalmanchey,[5] Gyorgy Fekete,[5] Alex Trojovsky,[6] Barbara Plecko,[7] Galen Breningstall,[8] Jun Tohyama,[9] Yoko Aoki,[1] and Yoichi Matsubara[1,10]

[1]*Department of Medical Genetics, Tohoku University School of Medicine, Sendai, Japan;* [2]*Division of Pediatric Neurology, Cincinnati Children's Hospital, Cincinnati, Ohio;* [3]*Discipline of Paediatrics and Child Health, University of Sydney and Royal Alexandra Hospital for Children, Westmead, Australia;* [4]*First Department of Pediatrics, Comenius University Children's Hospital, Bratislava, Slovakia;* [5]*Department of Pediatrics, Semmelweis University, Budapest, Hungary;* [6]*Institute for Medical Biology and Human Genetics, Medical University of Graz, Graz, Austria;* [7]*Department for Pediatrics, Medical University of Graz, Graz, Austria;* [8]*Department of Pediatrics (Neurology); Park Nicollet Clinic, Minneapolis, Minnesota;* [9]*Department of Pediatrics, Nishi-Niigata Chuo National Hospital, Niigata, Japan;* [10]*21st COE Program "Comprehensive Research and Education Center for Planning of Drug Development and Clinical Evaluation," Tohoku University, Sendai, Japan*

Communicated by Jan P. Kraus

Nonketotic hyperglycinemia (NKH) is an inborn error of metabolism characterized by accumulation of glycine in body fluids and various neurological symptoms. NKH is caused by deficiency of the glycine cleavage multi-enzyme system with three specific components encoded by *GLDC*, *AMT*, and *GCSH*. We undertook the first comprehensive screening for *GLDC*, *AMT*, and *GCSH* mutations in 69 families (56, six, and seven families with neonatal, infantile, and late-onset type NKH, respectively). *GLDC* or *AMT* mutations were identified in 75% of neonatal and 83% of infantile families, but not in late-onset type NKH. No *GCSH* mutation was identified in this study. *GLDC* mutations were identified in 36 families, and *AMT* mutations were detected in 11 families. In 16 of the 36 families with *GLDC* mutations, mutations were identified in only one allele despite sequencing of the entire coding regions. The *GLDC* gene consists of 25 exons. Seven of the 32 *GLDC* missense mutations were clustered in exon 19, which encodes the cofactor-binding site Lys754. A large deletion involving exon 1 of the GLDC gene was found in Caucasian, Oriental, and black families. Multiple origins of the exon 1 deletion were suggested by haplotype analysis with four *GLDC* polymorphisms. This study provides a comprehensive picture of the genetic background of NKH as it is known to date. Hum Mutat 27(4), 343–352, 2006. © 2006 Wiley-Liss, Inc.

KEY WORDS: GLDC; AMT; GCSH; glycine encephalopathy; nonketotic hyperglycinemia; NKH; glycine cleavage system; mutation spectrum; genotype–phenotype

INTRODUCTION

Nonketotic hyperglycinemia (NKH, MIM# 605899), also termed glycine encephalopathy, is an inborn error of amino acid metabolism characterized by the accumulation of a large amount of glycine in body fluids [Hamosh and Johnston, 2001]. Glycine levels are elevated to a much greater extent in cerebrospinal fluid (CSF) than in plasma; hence, an abnormally high value for the CSF/plasma glycine ratio is observed. NKH is clinically classified (by onset of symptoms) as three types: neonatal, infantile, or late-onset. Later onset appears to be associated with a better prognosis. The vast majority of patients fall into the neonatal category, which involves a stereotypic presentation with severe hypotonia, apnea requiring assisted ventilation, and intractable seizures. Approximately 30% of such patients die in the neonatal period. Survivors often have severe psychomotor retardation, although 15–20% of survivors achieve developmental milestones such as head control, independent sitting, or walking [Hoover-Fong et al., 2004]. Patients with the infantile type of NKH are often asymptomatic in the neonatal period and the phenotype is characterized by mild to moderate psychomotor retardation, behavioral problems, seizures, and chorea. The clinical presentations of late-onset NKH are heterogeneous. In previous studies, two families did not have seizures or mental retardation, but exhibited progressive paraplegia and optic atrophy [Bank and Morrow, 1972; Steiman et al., 1979]. Another family was reported to present with mental retardation and choreoathetosis [Singer et al., 1989].

The fundamental defect lies in the glycine cleavage system (GCS; EC2.1.2.10) [Tada et al., 1969]. The GCS is a mitochondrial complex enzyme system that consists of four

The Supplementary Material referred to in this article can be accessed at http://www.interscience.wiley.com/jpages/1059-7794/suppmat.

Received 11 July 2005; accepted revised manuscript 9 November 2005.

*Correspondence to: Shigeo Kure, M.D., Department of Medical Genetics, Tohoku University School of Medicine, 1-1 Seiryomachi, Aobaku, Sendai 980-8574, Japan.
E-mail: skure@mail.tains.tohoku.ac.jp

Grant sponsor: Ministry of Education, Culture, Sports, Science, and Technology; Ministry of Health, Labor, and Public Welfare in Japan.
DOI 10.1002/humu.20293
Published online 31 January 2006 in Wiley InterScience (www.interscience.wiley.com).

individual proteins [Kikuchi, 1973]: glycine decarboxylase (also called P-protein), aminomethyltransferase (T-protein), hydrogen carrier protein (H-protein), and dihydrolipoamide dehydrogenase (L-protein). The enzymatic analysis of NKH patients revealed that approximately 80% of patients with NKH have a *GLDC* deficiency and the rest have an *AMT* deficiency [Tada and Hayasaka, 1987]. Mitochondrial precursors of human P, T, H, and L-proteins consist of 1,020, 403, 173, and 509 amino acids, respectively. Dihydrolipoamide dehydrogenase is a housekeeping enzyme that serves as an E3 component of other α-keto acid dehydrogenase complexes, such as pyruvate dehydrogenase. Deficiency of dihydrolipoamide dehydrogenase causes progressive neurological deterioration with lactic acidosis but not hyperglycinemia [Hong et al., 1996]. The three GCS-specific components (P, T, and H-proteins) are encoded by distinct genes: *GLDC* (MIM# 238300) on chromosome 9p24 [Isobe et al., 1994], *AMT* on 3p21.1-21.2 [Nanao et al., 1994], and *GCSH* (MIM# 238330) on 16p24 [Kure et al., 2001], respectively.

To date, a limited number of NKH mutations have been reported (Human Gene Mutation Database, Cardiff; http://www.hgmd.cf.ac.uk). The *GLDC* mutations reported to date include the S564I mutation that is prevalent in Finnish patients [Kure et al., 1992], the R515S mutation found in 5% of Caucasian patients [Toone et al., 2000], microdeletions [Kure et al., 1991], large deletions [Takayanagi et al., 2000; Sellner et al., 2005], one abnormal splicing [Flusser et al., 2005], one nonsense mutation [Sellner et al., 2005], and 10 missense mutations [Toone et al., 2002; Korman et al., 2004; Kure et al., 2004; Boneh et al., 2005; Dinopoulos et al., 2005]. The *AMT* gene (MIM# 238310) mutations identified to date include nine missense mutations [Nanao et al., 1994, 1994a; Kure et al., 1998; Toone et al., 2000, 2001, 2003], one microdeletion [Kure et al., 1998, 1998b], and one splicing mutation [Toone et al., 2000]. In *GCSH* we have found one abnormal splicing in a patient with a transient form of NKH [Kure et al., 2002]. Since multiple genes are responsible for NKH, previous studies screened only a small number of *GLDC* and *AMT* exons and/or a few patients, which hampered elucidation of the genetic background of NKH.

The purpose of the present study was to establish the mutation spectrum of NKH by performing a comprehensive screening for mutations in *GLDC*, *AMT*, and *GCSH* in 69 families with three different types of NKH. The structure of *AMT* has been determined [Nanao et al., 1994, 1994b]. Also, we previously reported the exon-intron organizations of *GLDC* [Takayanagi et al., 2000] and *GCSH* [Kure et al., 2001], which provided us with basic information to amplify the entire coding regions for the three genes. To increase the sensitivity of mutational screening, we directly sequenced all amplicons without employing prescreening scanning methods such as single-strand conformation polymorphism.

MATERIALS AND METHODS

Patients

Patients were examined in the metabolic disease clinics of a number of referring hospitals. NKH was clinically suspected based on the presentation of symptoms characteristic of each disease type and electroencephalograms (EEG) recordings, and were subsequently confirmed by amino acid analysis. The CSF/serum glycine ratio at diagnosis was >0.04 in all patients, whereas it was <0.03 in normal neonates. Patients were classified into three clinical subtypes (neonatal, infantile, and late-onset) based on the onset of clinical symptoms.

Neonatal type. We studied 56 families with neonatal onset. Initial symptoms, including hypotonia, apnea, and coma, developed within 7 days after birth–in most cases within 3 days. Almost all of the patients showed a burst suppression pattern on EEG within 2 weeks after birth, and hypsarrhythmia thereafter.

Infantile type. Six families were enrolled. Symptoms started at 3–12 months of age. Five of the six patients had no symptoms in the neonatal period. Very mild hypotonia and apnea were observed in patient P107 [Dinopoulos et al., 2005]. Mild mental retardation and abnormal behaviors, such as aggressiveness, developed in adolescence.

Late-onset type. We studied seven patients with late-onset NKH. All seven patients had elevated glycine concentrations in repeated amino acid analysis of CSF and/or plasma. Spastic paraplegia without mental retardation developed in three of the seven patients. These patients resembled those in previously reported families [Bank and Morrow, 1972; Steiman et al., 1979]. The rest of the patients presented with mental retardation after they entered school or during adolescence. There is some confusion in terms of phenotypic classification of the mild form of the infantile type and the late-onset type, since there are some reports of patients in whom developmental delay or mild hypotonia started in the middle or late infantile periods [Flannery et al., 1983; Singer et al., 1989]. We classified such patients as having the infantile type—not the late-onset type. In the present study we classified patients as having the late-onset type when they were free of any symptoms during infancy.

Mutational Screening

Exons and flanking intron sequences of *GLDC* (GenBank NM_000170, NT_008413.16), *AMT* (GenBank NM_00481, NT_086638.1), and *GCSH* (GenBank NM_004483, NC_00016.8) were amplified by PCR from genomic DNA, followed by direct sequencing analysis using the dye-primer sequencing method as previously described [Kure et al., 2001]. The 18-mer oligonucleotides of the M13 and reverse sequencing primers were added to the 5′ end of the forward and reverse PCR primers, respectively. We initially screened for a large deletion involving *GLDC* exon 1 by semiquantitative PCR using the pseudogene of *GLDC* (*GLDCP*) as a gene dose control [Takayanagi et al., 2000]. PCR primer sequences for amplifying *GLDC* exons 1–6 were previously reported [Takayanagi et al., 2000], and those for other exons are described in Supplementary Table S1 (available online at http://www.interscience.wiley.com/jpages/1059-7794/suppmat). Each PCR cycle consisted of denaturing at 98°C for 10 sec, annealing at 55°C for 30 sec, and extension at 72°C for 30 sec, with repetition for 35 cycles. For PCR amplification of *GLDC* exon 1, 10% dimethylformamide was added to the reaction mixture. Fifty control subjects were subsequently screened for any detected base changes to exclude noncausative polymorphisms. If no mutations were detected in the sequencing analysis of *GLDC*, we screened for mutations in *AMT* by amplifying all of the nine exons. When no mutations were identified in either *GLDC* or *AMT*, we sequenced all of the five exons in *GCSH*. For characterization of *GLDC* and *AMT* missense mutations, each mutated amino acid residue was compared with the corresponding amino acid in rat [Sakata et al., 2001], chicken [Kume et al., 1991], pea [Turner et al., 1992], and *E. coli* [Okamura-Ikeda et al., 1993], as shown in Tables 2 and 3.

Characterization of the *GLDC* Deletion

We identified the minimum deleted region of both alleles of each homozygous patient of the *GLDC* exon 1 deletion. Fifteen sequence tagged sites (STSs) were used for this deletion mapping,

as illustrated in Fig. 1. PCR primer sequences and amplification conditions for D9S281 and RH92434 were obtained from the website of the UCSC Genome Browser (http://genome.ucsc.edu). The PCR primer sequences and amplicon sizes of STSs 1–8 are presented in Supplementary Table S1. STSs 1–7 were located 5′ upstream of the *GLDC* gene, and STS 8 was located in intron 2. Amplification primers for *GLDC* exons 1–5 were also used in the deletion mapping. We amplified these 15 STSs by using genomic DNA of Patients P5 and P36 as a template in order to test whether each STS was involved in the homozygously deleted region. Structural information about the 5′ upstream region of *GLDC* and the location of *Alu* motifs was obtained from the UCSC Genome Browser (Fig. 1).

RESULTS

Mutation Screening

We performed mutational screening in 69 NKH families (56 neonatal type, six infantile type, and seven late-onset type). First, the *GLDC* exon 1 deletion was screened by semiquantitative PCR amplification using the *GLDCP* as a control of the gene copy number. This deletion was found in six families (Table 1). Subsequent extensive sequencing of *GLDC*, *AMT*, and *GCSH* coding exons revealed that 42 of the 56 neonatal-type families (75%) had *GLDC* or *AMT* mutations in at least one of two alleles. *GLDC* mutations were found in 31 (74%) and *AMT* mutations were detected in 11 (26%) of the 42 families. No differences were

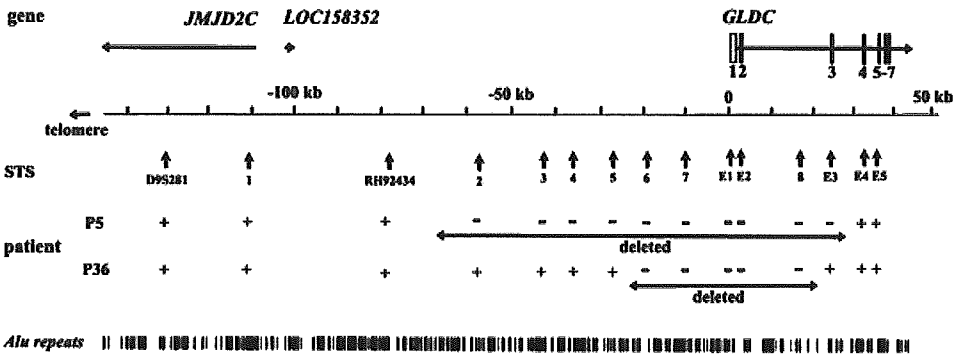

FIGURE 1. **Mapping of the *GLDC* deletions. Genomic regions that were homozygously deleted in patients P5 and P36 were defined by amplification of 13 STS markers. The JMJD2C gene and the gene-like structure, LOC158352, are shown based on the information of the UCSC Genome Browser. E1–5 indicate amplicons including the *GLDC* exons 1–5, respectively. Amplicons (+) indicate that the STS was successfully amplified, while (–) means that the STS failed to be amplified.**

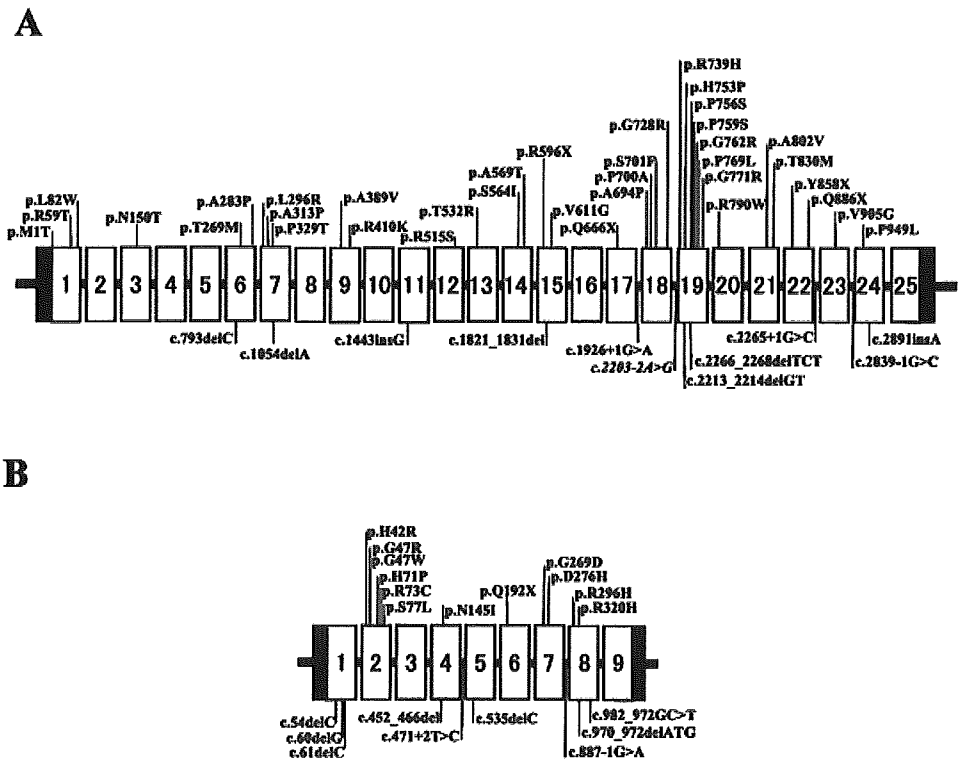

FIGURE 2. **NKH mutations identified in this and previous studies. The *GLDC* (A) and *AMT* (B) exons are indicated by open boxes, and noncoding regions are shaded. Missense and nonsense mutations are shown above the exon boxes, and deletions/insertions and mutations of splicing errors are indicated below the exon boxes.**

TABLE 1. Patients With *GLDC* or *AMT* Mutations

						Mutation[a]			
Family number	Ethnicity	Age of onset	Consanguinity	CSF Gly (mM)	CSF/serum Gly ratio	Gene	Mutation 1	Mutation 2	Reference
Neonatal type									
P14	Caucasian	Day 1	No	296	0.25	*GLDC*	Exon 1 deletion	c.2714T>G	This study
P21	Caucasian	Day 1	Yes	71	0.24	*AMT*	c.230C>T	c.230C>T	This study
P26	Caucasian	Day 1	Yes	86	0.27	*AMT*	c.125A>G	c.125A>G	Kure et al. [1998a]
P29	Caucasian	Day 1	No	43	0.04	*GLDC*	c.793delC	ND	This study
P31	Caucasian	Day 1	No	196	0.26	*AMT*	c.471+2T>C	c.887G>A	This study
P32	Caucasian	Day 1	No	32	0.20	*GLDC*	c.1786C>T	c.1786C>T	This study
P36	Caucasian	Day 1	No	220	0.18	*GLDC*	Exon 1 deletion	Exon 1 deletion	This study
P39	Caucasian	Day 1	No	187	0.13	*GLDC*	c.1595C>G	c.1832T>G	This study
P48	Caucasian	Day 1	No	198	0.20	*GLDC*	c.2665+1G>C	ND	This study
P49	Caucasian	Day 1	No	213	0.17	*GLDC*	c.2203–2A>G	ND	This study
P59	Caucasian	Day 1	Yes	202	0.23	*GLDC*	c.1996C>T	c.1996C>T	This study
P5	Oriental	Day 1	No	240	0.18	*GLDC*	Exon 1 deletion	Exon 1 deletion	Ohya et al. [1991]
P6	Oriental	Day 1	No	160	0.09	*GLDC*	c.245T>G	c.1821_18311del	Kure et al. [2004]
P19	Oriental	Day 1	No	264	0.30	*GLDC*	c.449A>C	c.2368C>T	Kure et al. [2004]
P25	Oriental	Day 1	No	74	0.34	*AMT*	c.54delC	c.826G>C	Kure et al. [1998b]
P74	Oriental	Day 1	No	117	0.12	*GLDC*	c.2311G>A	ND	This study
P86	Oriental	Day 1	No	177	0.20	*GLDC*	c.2213_2214delGT	ND	This study
P93	Oriental	Day 1	No	130	0.13	*GLDC*	c.2105C>T	ND	This study
P115	Oriental	Day 1	No	145	0.11	*AMT*	c.147delG	c.970_972delATG	This study
P124	Oriental	Day 1	No	300	0.11	*GLDC*	c.255+1G>A	c.806C>T	This study
P30	Caucasian	Day 2	No	121	0.19	*AMT*	c.60delG	c.471+2T>C	This study
P44	Caucasian	Day 2	No	98	0.11	*GLDC*	c.806C>T	c.255+1G>A	This study
P46	Caucasian	Day 2	No	155	0.13	*GLDC*	c.2293C>T	c.1705G>A	This study
P47	Caucasian	Day 2	No	78	0.17	*GLDC*	c.2519T>A	ND	This study
P61	Caucasian	Day 2	No	186	0.17	*AMT*	c.982_972GC>T	c.452_466del	This study
P75	Caucasian	Day 2	No	167	0.16	*AMT*	c.212A>C	c.217C>T	This study
P3	Oriental	Day 2	No	151	0.10	*GLDC*	c.2306C>T	c.2846C>T	This study
P4	Oriental	Day 2	No	387	0.28	*GLDC*	c.2258A>C	c.2839–1G>C	This study
P7	Oriental	Day 2	No	164	0.10	*GLDC*	c.2266_2268delTTC	ND	Kure et al. [1991]
P8	Oriental	Day 2	No	209	0.31	*GLDC*	c.2080G>C	ND	This study
P10	Oriental	Day 2	No	517	0.20	*GLDC*	c.887T>G	ND	This study
P77	Oriental	Day 2	No	148	0.12	*GLDC*	c.449A>C	c.1926+1G>A	This study
P91	Oriental	Day 2	No	132	0.08	*AMT*	c.61delC	c.535delC	This study
P69	Oriental	Day 3	No	220	0.12	*GLDC*	c.2311G>A	ND	This study
P70	Oriental	Day 3	No	68	0.19	*GLDC*	Exon 1 deletion	ND	This study
P120	Oriental	Day 3	No	324	0.19	*GLDC*	c.2574T>G	ND	This study
P23	Oriental	Day 4	No	83	0.14	*GLDC*	c.2182G>C	ND	This study
P104	Caucasian	Day 4	No	240	0.26	*GLDC*	c.1166C>T	c.1443insG	This study
P15	Black	Day 5	No	333	0.08	*GLDC*	Exon 1 deletion	c.2891insA	This study
P34	Caucasian	Day 6	No	174	0.08	*AMT*	c.139G>T	ND	This study
P76	Caucasian	Day 6	No	215	0.18	*AMT*	c.136G>A	c.230C>T	This study
P72	Black	Day 7	No	117	0.20	*GLDC*	c.2665+1G>C	c.176G>C	This study
Infantile type									
P50	Caucasian	3 months	No	200	0.25	*GLDC*	Exon 1 deletion	c.2311G>A	This study
P78	Caucasian	6 months	No	46	0.06	*GLDC*	c.2216G>A	c.2216G>A	Dinopoulos et al. [2005]
P12	Caucasian	12 months	No	41	0.04	*GLDC*	c.2216G>A	ND	Christodoulou et al. [1993]
P107	Caucasian	Unclear[b]	No	150	0.09	*GLDC*	c.1166C>T	c.1166C>T	Dinopoulos et al. [2005]
P108	Caucasian	Unclear[b]	No	55	0.05	*GLDC*	c.1166C>T	c.1166C>T	Dinopoulos et al. [2005]

[a]DNA mutation numbering is based on cDNA sequence: +1 corresponds to the A of the ATG translation initiation codon. *GLDC*: NM_000170; *AMT*: NM_00481.
[b]Developmental delay in infantile period.
ND, not detected.

TABLE 2. *GLDC* Mutations*

Mutation	Location	Consequence of mutation	No. of families	Novel mutation	Comments				
Missense mutations					Evolutionary conservation				
					Human	Rat	Chicken	Pea	*E.coli*
c.176G>C	Exon 1	p.R59T	1	Yes	Arg	Arg	Arg	Ser	Ser
c.245T>G	Exon 1	p.L82W	1	No	Lue	Lue	Val	Val	Val
c.449A>C	Exon 3	p.N150T	2	No	Asn	Asn	Asn	Asn	Asn
c.806C>T	Exon 6	p.T269M	2	Yes	Thr	Thr	Thr	Thr	Thr
c.887T>G	Exon 7	p.L296R	1	Yes	Leu	Leu	Leu	Leu	Ile
c.1166C>T	Exon 9	p.A389V	3	No	Ala	Ala	Ala	Ala	Ala
c.1595C>G	Exon 13	p.T532R	1	Yes	Thr	Thr	Thr	His	Thr
c.1705G>A	Exon 14	p.A569T	1	Yes	Ala	Ala	Ala	Met	Ile
c.1832T>G	Exon 15	p.V611G	1	Yes	Val	Val	Ile	Phe	Val
c.2080G>C	Exon 18	p.A694P	1	Yes	Ala	Ala	Ala	Ala	Cys
c.2105C>T	Exon 18	p.S701F	1	Yes	Ser	Ser	Ser	Ser	Ser
c.2182G>C	Exon 18	p.G728R	1	Yes	Gly	Gly	Gly	Gly	Gly
c.2216G>A	Exon 19	p.R739H	2	No	Arg	Arg	Arg	Ser	Ser
c.2258A>C	Exon 19	p.H753P	1	Yes	His	His	His	His	His
c.2293C>T	Exon 19	p.P765S	1	Yes	Pro	Pro	Pro	Pro	Pro
c.2306C>T	Exon 19	p.P769L	1	Yes	Pro	Pro	Pro	Pro	Pro
c.2311G>A	Exon 19	p.G771R	3	Yes	Gly	Gly	Gly	Gly	Gly
c.2368C>T	Exon 20	p.R790W	1	No	Arg	Arg	–	–	–
c.2519T>A	Exon 21	p.M840K	1	Yes	Met	Met	Met	Met	Ile
c.2714T>G	Exon 23	p.V905G	1	Yes	Val	Val	Ile	Ile	Val
c.2846C>T	Exon 24	p.P949L	1	Yes	Pro	Pro	Pro	Pro	Pro
Nonsense mutations									
c.1786C>T	Exon 15	p.R596X	1	Yes					
c.1996C>T	Exon 17	p.Q666X	1	Yes					
c.2574T>G	Exon 22	p.Y858X	1	Yes					
Deletions and insertions									
Exon 1 deletion	Exon 1	Deletion including exon 1	6	No	A recurrent mutation				
c.793delC	Exon 6	Deletion of first letter of 265Gln codon	1	Yes	FS after codon 264/TRM at codon 296				
c.1821_1831del	Exon 15	11-bp deletion started at third letter of 607Gly codon	1	No	FS after codon 607/TRM at codon 669				
c.1443insG	Exon 11	Insertion of G after third letter of 481Leu codon	1	Yes	FS at codon 482/TRM at codon 491				
c.2213_2214delGT	Exon 19	Deletion of GT in 738Cys codon	1	Yes	FS after codon 738/TRM at codon 745				
c.2266_2268delTTC	Exon 19	Deletion of TTC in 756Phe codon	1	No	No FS/TRM at codon 1019				
c.2891insA	Exon 24	Insertion of A after second letter of 964Tyr codon	1	Yes	No FS/TRM at codon 964				
Aberrant splicing									
c.255+1G>A	Intron 2	Disruption of splicing donor site, gt>at	1	Yes					
c.1926+1G>A	Intron 17	Disruption of splicing donor site, gt>at	1	Yes					
c.2203-2A>G	Intron 18	Disruption of splicing acceptor site, ag>gg	1	Yes					
c.2665+1G>C	Intron 22	Disruption of splicing donor site, gt>ct	2	Yes					
c.2839-1G>C	Intron 23	Disruption of splicing acceptor site, ag>cg	1	Yes					

*DNA mutation numbering is based on cDNA sequence: +1 corresponds to the A of the ATG translation initiation codon. *GDLC*: NM_000170.
FS, frameshift; TRM, termination codon.

observed in CSF glycine levels between 42 mutation-positive and 14 mutation-negative individuals. *GLDC* mutations were detected in five (83%) of the six patients with infantile NKH. No mutations were found in *GLDC*, *AMT*, or *GCSH* in any of seven patients with late-onset NKH. NKH mutations were highly heterogeneous. Only nine of the 47 mutation-positive individuals were homozygous for a single mutation (three individuals from consanguineous families (P21, P26, and P59), and five homozygotes of recurrent mutations (P36, P5, P78, P107, and P108)). Patient P32 was homozygous for a private mutation (p.R596X), even though there was no evidence that he was the product of a consanguineous marriage. No *GCSH* mutations were identified in this study.

TABLE 3. *AMT* Mutations*

Mutation	Location	Sequence alternation	No. of families	Novel mutation	Comments				
Missense mutations					Evolutionary Conservation				
					Human	Rat	Chicken	Pea	*E.coli*
c.125A>G	Exon 2	p.H42R	1	No	His	His	His	His	His
c.136G>A	Exon 2	p.G47R	1	Yes	Gly	Gly	Gly	Gly	Ala
c.139G>T	Exon 2	p.G47W	1	Yes	Gly	Gly	Gly	Gly	Ala
c.212A>C	Exon 2	p.H71P	1	Yes	His	His	His	Asn	Ala
c.217C>T	Exon 2	p.R73C	1	Yes	Arg	Arg	Arg	Arg	Arg
c.230C>T	Exon 2	p.S77L	1	Yes	Ser	Ser	Ser	Ser	Gly
c.826G>C	Exon 7	p.D276H	1	No	Asp	Asp	Asp	Asp	Glu
c.887G>A	Exon 8	p.R296H	1	No	Arg	Arg	Lys	Arg	Lys
Deletions and insertion									
c.54delC	Exon 1	Deletion of third letter of 18Phe codon	1	No	FS at codon 20/TRM at codon 95				
c.60delG	Exon 1	Deletion of third letter of 20Pro codon	1	Yes	FS at codon 21/TRM at codon 95				
c.61delC	Exon 1	Deletion of first letter of 21Ala codon	1	Yes	FS at codon 21/TRM at codon 95				
c.147delG	Exon 2	Deletion of third letter of 49Met codon	1	Yes	FS at codon 50/TRM at codon 95				
c.452_466del	Exon 4	Deletion start at second letter of 151Lys codon	1	Yes	No FS/TRM at codon 398				
c.535delC	Exon 5	Deletion of first letter of 179Leu codon	1	Yes	FS at codon 179/TRM at codon 180				
c.970_972delATG	Exon 8	Deleion of 320Met codon	1	Yes	No FS/TRM at codon 482				
c.982_972GC>T	Exon 8	GC in 328Ala codon was substitued byT	1	Yes	FS at codon 328/TRM at codon 337				
Aberrant splicing									
c.471+2T>C	Intron 4	Disruption of splicing donor site, gt>gc	2	Yes					

*DNA mutation numbering is based on cDNA sequence: +1 corresponds to the A of the ATG translation initiation codon. *AMT*: NM_00481. FS, frameshift; TRM, termination codon.

GLDC Mutations

Deletion of exon 1 was detected in six patients (four Caucasian, one oriental, and one black). In this study we identified 36 *GLDC* mutations, 28 of which were novel (Table 2). None of the identified mutations were detected in 100 control alleles. There were 21 missense mutations, three nonsense mutations, seven deletion/insertion mutations, and five splicing mutations Table 3. For all of the 21 missense mutations the substituted amino acids are conserved in rats, and 13 of the 21 amino acids are conserved from humans to *E. coli*. Such a high degree of evolutionary conservation presumably reflects the functional importance of each of these amino acids. Seven mutations were found in multiple individuals with no apparent relationship. A missense mutation p.N150T was identified in oriental families, while p.T269M, p.A389V, p.R739H, and c.2665+1G>C were found in Caucasian families. Sequencing analysis of the *GLDC* gene revealed the presence of several polymorphisms, which were also found in control subjects (Table 4). Five of the polymorphisms were found in at least 10% of the control alleles tested. Three of them were found within exons (exon 1: c.249G>A; exon 4, c.501G>A; and exon 25, c.3070C>G (3′ noncoding region)). Two of them were located in introns (intron 9, c.1262+36A>G; and intron 19, c.2203-6insA). The c.2203-6insA polymorphism was located at the intron 19/exon 20 boundary, and substitutes the ttaaaaaaaatacag/GAAGAAA (A8 allele) to the ttaaaaaaaaatacag/GAAGAAA (A9 allele). Other polymorphisms that were less frequently observed were c.438G>A (p.T146T) in exon 3, c.1261+36A>G (intron 9), and c.1261+52G>A (intron 9).

AMT Mutations

A total of 17 mutations (including 13 novel mutations) were identified, including eight missense mutations, eight deletion/insertion mutations, and one splicing mutation. The evolutionary conservation of each mutated amino acid is shown in Table 3. All of these amino acids are conserved among humans, rats, and chickens, and six of eight amino acids are also conserved in peas, which suggests that they are functionally important. All of the deletion/insertion mutations generated a profoundly truncated AMT polypeptide. Two polymorphic sites were observed in two *AMT* exons: exon 2, c.327T>C; and exon 8, c.1083G>A.

Characterization of the *GLDC* Exon 1 Deletion

To define the boundaries of the exon 1 deletions, eight STSs were designed: seven STSs at the region 150 kb upstream of *GLDC*, and one STS in intron 2 of *GLDC* (Fig. 1; Supplementary Table S1). Two additional published STSs (D9S281 and RH92434) and *GLDC* exons 1–5 were also used for the deletion mapping. We amplified a total of 15 STSs using genomic DNA as the templates obtained from Patients P5 and P36, who were homozygous for the *GLDC* exon 1 deletion. In Patient P5, STSs 2–8 and exons 1–3 were not amplified, indicating that the 80–100 kb was homozygously deleted. In Patient P36, STSs 6–8, and exons 1–2 failed to be amplified, demonstrating a 35–45 kb homozygous deletion. Both deletions did not extend to a known gene 5′ adjacent to *GLDC*: jumonji domain containing protein2C (*JMJD2C*). *Alu* repeats in this region were identified using the UCSD Genome Browser (Fig. 1).

TABLE 4. Haplotype Analysis of the *GLDC* Allele With the Exon 1 Deletion

			Polymorphic site			
Patients	Ethnicity	Allele	Exon 4 c.501G>A[a]	Intron 9 c.1262+36A>G	Intron 19 c.2203–6insA	Exon 25 (3′ noncoding region) c.3070C>G
P5	Oriental	Allele 1	G	A	A8	C
		Allele 2	G	A	A8	C
P14	Caucasian	Allele 1	G	A	A8	C
P36	Caucasian	Allele 1	G	A	A8	C
		Allele 2	G	A	A9	C
P50	Caucasian	Allele 1	A	G	A9	C

[a]DNA mutation numbering is based on cDNA sequence: +1 corresponds to the A of the ATG translation initiation codon. *GDLC*: NM_000170.

Haplotype Analysis of the *GLDC* Mutations

The identification of five polymorphisms within *GLDC* allowed us to determine the haplotypes of the mutant alleles with the exon 1 deletion. Haplotypes of the deletion allele were identified in four families (P5, P14, P36, and P50), but could not be determined in two families (P15 and P86; Table 4). Four mutant alleles shared the same haplotype (G, A, A8, C), with the genotypes of four polymorphic sites being written as follows: (c.501G>A, c.1232+36A>G, c.2203-6ins A, c3070C>G). Two additional haplotypes, (G, A, A9, C) and (A, G, A9, C) were also found, suggesting multiple origins of the exon 1 deletion.

Mutation Spectra of the *GLDC* and *AMT* Genes

The *GLDC* mutations detected in this study, as well as those from previous reports, are illustrated in Fig. 2A. The most striking feature of the mutation distribution is the clustering of the missense mutations in exon 19. Seven of the 32 missense mutations (22%) were identified in exon 19. The distribution of the *AMT* mutations is shown in Fig. 2B. No obvious clustering of the mutations was found in this gene.

DISCUSSION

We undertook an extensive screening for *GLDC*, *AMT*, and *GCSH* mutations in a cohort of patients with NKH, and the results reveal a comprehensive picture of the mutation spectrum of NKH to date. In this study, 36 *GLDC* mutations and 17 *AMT* mutations were detected, including 28 novel *GLDC* and 13 novel *AMT* mutations. In total, 75% of neonatal and 83% of infantile patients were positive for *GLDC* or *AMT* mutations. Mutations in NKH patients were highly heterogeneous. Patients were found to be compound heterozygotes in 38 of 47 mutation-positive cases (81%). This is in sharp contrast with findings in countries with a high incidence of NKH, such as Finland [von Wendt et al., 1979] and Israel [Korman and Gutman, 2002]. In those countries there are common mutations and many homozygotes for each common mutation. A *GLDC* missense mutation (p.564I) has been identified in Finland [Kure et al., 1992], and a *GLDC* missense mutation (p.M1 T) and *AMT* missense mutation (p.H42R) have been found in Israel [Boneh et al., 2005; Flusser et al., 2005].

In 16 of 36 families (44%) with *GLDC* mutations, we were able to identify a mutation in only one of two mutant alleles despite extensive mutational screening of *GLDC*, *AMT*, and *GCSH*. Mutations may present in promoter regions or introns of the GLDC gene, or large deletions or duplications may exist. Deletion of *GLDC* exon 1 was detected in eight of the 36 families (22%) with GLDC mutations. The deletion was found in Caucasian, oriental, and black patients. Subsequent haplotype analysis suggested multiple origins of the deletion. There is a high-density repeat region of *Alu* motifs in the 5′ upstream region and the introns of *GLDC*, which are reported to trigger a homologous recombination between two *Alu* motifs and cause a large deletion (e.g., the C1-inhibitor gene, *C1-INH* [Stoppa-Lyonnet et al., 1991]; lysyl hydroxylase gene, *PLOD1* [Pousi et al., 1994]; and a MutL mismatch repair gene, *hMLH1* [Mauillon et al., 1996]). We therefore speculate that the deletions of *GLDC* exon 1 are caused by homologous recombination between *Alu* repeats. Recently, Sellner et al. [2005] reported a deletion of *GLDC* exons 2–15 that was flanked by *Alu* motifs. *Alu*-mediated homologous deletion may occur not only in the 5′ region of *GLDC*, but also in other regions of *GLDC*.

No mutations were detected in seven patients with late-onset NKH, despite intensive screening of the entire coding regions of *GLDC*, *AMT*, and *GCSH*, which suggests that gene(s) other than GCS genes may be responsible for late-onset NKH. Several reports have described hyperglycinemic patients with no evidence of neurological symptoms until 1 year of age [Bank and Morrow, 1972; Steiman et al., 1979; Lane et al., 1991, 1998; Wiltshire et al., 2000; Ellaway et al., 2001]. The diagnosis of NKH was not confirmed by mutational analysis in any of those patients. Patients with atypical GE tend to have a relatively modest elevation of serum and CSF glycine concentrations, which may be also caused by other genetic disorders or therapeutic agents [Korman and Gutman, 2002]. Vanishing white matter disease is a type of leukoencephalopathy with characteristic MRI findings that is commonly associated with mild elevation of CSF glycine concentration [van der Knaap et al., 1999]. This disorder might have been classified as a late-onset NKH if the responsible genes (*EIF2B5* and *EIF2B2*) had not been identified [Leegwater et al., 2001]. For a more accurate diagnosis and better understanding of late-onset NKH patients, genetic characterization is of paramount importance. There are several other proteins that are functionally related to the GCS reaction. Lipoylation of H-protein is catalyzed by lipolyltransferase. The gene encoding the enzyme would be a good candidate for NKH [Fujiwara et al., 1999]. Two types of glycine transporters, GlyT1 and GlyT2, have been identified [Zafra et al., 1997]. GlyT2 is located only in the brain stem and spinal cord, while GlyT1 is distributed in the brain, kidney, and liver, and the latter transporter may have a role in maintaining the glycine level in both CSF and plasma. Thus, the GlyT1 gene is another good candidate gene for NKH.

A mutation in at least one of two alleles was identified in 47 of 62 patients with neonatal or infantile type NKH, 36 of whom (77%) had *GLDC* mutations. The dominance of the *GLDC* mutations over *AMT* mutations is in agreement with previous

enzymatic studies [Tada and Hayasaka, 1987; Toone et al., 2000]. No *GCSH* mutations were identified in any of the three clinical subtypes of NKH, suggesting that *GCSH* mutations are extremely rare in NKH. We recently identified a heterozygous splicing mutation in *GCSH* in a Japanese family with a peculiar type of NKH–transient type NKH [Kure et al., 2002]. Transient NKH is indistinguishable from neonatal NKH in terms of the onset of disease, but serum and CSF glycine are normalized within 2–8 weeks [Luder et al., 1989; Schiffmann et al., 1989]. A girl with atypical NKH was reported to have low enzymatic activity of the H-protein [Hiraga et al., 1981]. Unlike other patients with NKH, this patient showed progressive deterioration and extensive spongy degeneration of white matter with marked gliosis on postmortem examination [Trauner et al., 1981]. It may be that *GCSH* mutations will be found in patients with atypical NKH rather than the more readily recognized clinical form of NKH.

Seven of 32 *GLDC* missense mutations were clustered in exon 19 (Fig. 2). Glycine decarboxylase consists of 1,020 amino acids, and exon 19 encodes 37 of 1,020 amino acids (3.6%), that is, 22% of the *GLDC* missense mutations were clustered in only 3.6% of the protein-coding region. Two octapeptides encoded in exon 19–His749 to Phe756 (HLNLHKTF) and Pro759 to Gly766 (PHGGGGPG)–are perfectly conserved in humans, chickens, peas, and *E. coli*. Crystal structure analysis revealed that His749, Asn751, His753, Lys754, and His760 (underlined) formed an active-site pocket of the GLDC enzyme [Nakai et al., 2005], and the cofactor of GLDC, pyridoxal phosphate, was covalently bound to Lys754 [Fujiwara et al., 1987]. Amino acid changes in this conserved region frequently abolish GLDC enzyme activity, which may be a possible explanation for the high incidence of *GLDC* missense mutations in this region.

Patients P107 and P108 were homozygous for the p.A389V mutation, while patient P104 was a compound heterozygote of the p.A389V mutation and a null mutation, c.1443insG (Table 1). The p.A389V mutation had approximately 8% residual activity in the COS7 expression analysis [Dinopoulos et al., 2005]. Patients P107 and P108 did not present with comas or seizures in the neonatal period, but exhibited developmental delay and abnormal behaviors that developed with age. In contrast, Patient P104 had a typical presentation of the neonatal form of NKH, but subsequently the course of the disease was less severe. The presence of the pA389V mutant allele, which allows some residual enzyme activity, may explain this milder phenotype of classic NKH. The clinical course of P104 resembled those of P6 and P19, who were expected to have 5–8% residual activity by the in vitro expression analysis [Kure et al., 2004]. These results suggest that only a few-percent difference in GCS residual activity dramatically alters the clinical picture, such as age of onset and prognosis. A previous enzymatic study of patients with neonatal and infantile NKH supports this suggestion [Hayasaka et al., 1987]. GCS activities ranged from 0 to 0.7 nmoles of CO_2 formed/mg protein/hr in the neonatal type, while it ranged from 0.7 to 1.4 in the infantile type (for which the control range was 3.9–5.2). However, an exception was observed. Both P69 and P50 were compound heterozygotes of *GLDC* exon 1 deletion and p.G771R. Patient P69 manifested typical symptoms on the second day of life, whereas Patient P50 did not develop symptoms until 3 months of age. Thus far, residual activity is a major determinant of the clinical course, but it is probably modified by environmental factors and/or genotypes of other than the GCS genes.

Elucidation of the responsible gene(s) for late-onset NKH, and screening for deletions in all *GLDC* exons are needed to establish a more complete picture of the genetic background and develop the genotype–phenotype relationships in NKH.

ACKNOWLEDGMENTS

We are grateful to the families who participated in this work. We thank Dr. Avihu Boneh (Royal Children's Hospital, Melbourne), Dr. Helena Haekansson (Lalmar Central Hospital, Sweden), Dr. Shiro Tono-Oka (Kagoshima City Hospital, Japan), Dr. Toshimitsu Takayanagi (National Hospital Organization Saga National Hospital, Japan), Dr. Mitsuru Kubota (Hokkaido University Hospital, Japan), and Dr. Masaki Takayanagi (Chiba Children's Hospital, Japan) for referring the NKH patients.

REFERENCES

Bank WJ, Morrow G 3rd. 1972. A familial spinal cord disorder with hyperglycinemia. Arch Neurol 27:136–144.

Boneh A, Korman SH, Sato K, Kanno J, Matsubara Y, Lerer I, Ben-Neriah Z, Kure S. 2005. A single nucleotide substitution that abolishes the initiator methionine codon of the GLDC gene is prevalent among patients with glycine encephalopathy in Jerusalem. J Hum Genet 50:230–234.

Christodoulou J, Kure S, Hayasaka K, Clarke JT. 1993. Atypical nonketotic hyperglycinemia confirmed by assay of the glycine cleavage system in lymphoblasts. J Pediatr 123:100–102.

Dinopoulos A, Kure S, Chuck G, Sato K, Gilbert DL, Matsubara Y, Degrauw T. 2005. Glycine decarboxylase mutations: a distinctive phenotype of nonketotic hyperglycinemia in adults. Neurology 64:1255–1257.

Ellaway CJ, Mundy H, Lee PJ. 2001. Successful pregnancy outcome in atypical hyperglycinaemia. J Inherit Metab Dis 24: 599–600.

Flannery DB, Pellock J, Bousounis D, Hunt P, Nance C, Wolf B. 1983. Nonketotic hyperglycinemia in two retarded adults: a mild form of infantile nonketotic hyperglycinemia. Neurology 33: 1064–1066.

Flusser H, Korman SH, Sato K, Matsubara Y, Galil A, Kure S. 2005. Mild glycine encephalopathy (NKH) in a large kindred due to a silent exonic GLDC splice mutation. Neurology 64: 1426–1430.

Fujiwara K, Okamura-Ikeda K, Motokawa Y. 1987. Amino acid sequence of the phosphopyridoxyl peptide from P-protein of the chicken liver glycine cleavage system. Biochem Biophys Res Commun 149:621–627.

Fujiwara K, Suzuki M, Okumachi Y, Okamura-Ikeda K, Fujiwara T, Takahashi E, Motokawa Y. 1999. Molecular cloning, structural characterization and chromosomal localization of human lipoyltransferase gene. Eur J Biochem 260:761–767.

Hamosh A, Johnston MV. 2001. Nonketotic hyperglycinemia. In: Scriver CR, Beaudet AL, Sly WS, Valle D, editors. The metabolic and molecular bases of inherited disease, vol 2. New York: McGraw-Hill. p 2065–2078.

Hayasaka K, Tada K, Fueki N, Nakamura Y, Nyhan WL, Schmidt K, Packman S, Seashore MR, Haan E, Danks DM, Schutgems RBH. 1987. Nonketotic hyperglycinemia: analyses of glycine cleavage system in typical and atypical cases. J Pediatr 110:873–877.

Hiraga K, Kochi H, Hayasaka K, Kikuchi G, Nyhan WL. 1981. Defective glycine cleavage system in nonketotic hyperglycinemia. Occurrence of a less active glycine decarboxylase and an abnormal aminomethyl carrier protein. J Clin Invest 68: 525–534.

Hong YS, Kerr DS, Craigen WJ, Tan J, Pan Y, Lusk M, Patel MS. 1996. Identification of two mutations in a compound heterozygous child with dihydrolipoamide dehydrogenase deficiency. Hum Mol Genet 5:1925–1930.

Hoover-Fong JE, Shah S, Van Hove JL, Applegarth D, Toone J, Hamosh A. 2004. Natural history of nonketotic hyperglycinemia in 65 patients. Neurology 63:1847–1853.

Isobe M, Koyata H, Sakakibara T, Momoi-Isobe K, Hiraga K. 1994. Assignment of the true and processed genes for human glycine decarboxylase to 9p23-24 and 4q12. Biochem Biophys Res Commun 203:1483–1487.

Kikuchi G. 1973. The glycine cleavage system: composition, reaction mechanism, and physiological significance. Mol Cell Biochem 1:169–187.

Korman SH, Gutman A. 2002. Pitfalls in the diagnosis of glycine encephalopathy (non-ketotic hyperglycinemia). Dev Med Child Neurol 44:712–720.

Korman SH, Boneh A, Ichinohe A, Kojima K, Sato K, Ergaz Z, Gomori JM, Gutman A, Kure S. 2004. Persistent NKH with transient or absent symptoms and a homozygous GLDC mutation. Ann Neurol 56:139–143.

Kume A, Koyata H, Sakakibara T, Ishiguro Y, Kure S, Hiraga K. 1991. The glycine cleavage system. Molecular cloning of the chicken and human glycine decarboxylase cDNAs and some characteristics involved in the deduced protein structures. J Biol Chem 266:3323–3329.

Kure S, Narisawa K, Tada K. 1991. Structural and expression analyses of normal and mutant mRNA encoding glycine decarboxylase: three-base deletion in mRNA causes nonketotic hyperglycinemia. Biochem Biophys Res Commun 174: 1176–1182.

Kure S, Takayanagi M, Narisawa K, Tada K, Leisti J. 1992. Identification of a common mutation in Finnish patients with nonketotic hyperglycinemia. J Clin Invest 90:160–164.

Kure S, Mandel H, Rolland MO, Sakata Y, Shinka T, Drugan A, Boneh A, Tada K, Matsubara Y, Narisawa K. 1998a. A missense mutation (His42Arg) in the T-protein gene from a large Israeli-Arab kindred with nonketotic hyperglycinemia. Hum Genet 102:430–434.

Kure S, Shinka T, Sakata Y, Osamu N, Takayanagi M, Tada K, Matsubara Y, Narisawa K. 1998b. A one-base deletion (183delC) and a missense mutation (D276H) in the T-protein gene from a Japanese family with nonketotic hyperglycinemia. J Hum Genet 43:135–137.

Kure S, Kojima K, Kudo T, Kanno K, Aoki Y, Suzuki Y, Shinka T, Sakata Y, Narisawa K, Matsubara Y. 2001. Chromosomal localization, structure, single-nucleotide polymorphisms, and expression of the human H-protein gene of the glycine cleavage system (GCSH), a candidate gene for nonketotic hyperglycinemia. J Hum Genet 46:378–384.

Kure S, Kojima K, Ichinohe A, Maeda T, Kalmanchey R, Fekete G, Berg SZ, Filiano J, Aoki Y, Suzuki Y, Izumi T, Matsubara Y. 2002. Heterozygous GLDC and GCSH gene mutations in transient neonatal hyperglycinemia. Ann Neurol 52:643–646.

Kure S, Ichinohe A, Kojima K, Sato K, Kizaki Z, Inoue F, Yamanaka C, Matsubara Y. 2004. Mild variant of nonketotic hyperglycinemia with typical neonatal presentations: mutational and in vitro expression analyses in two patients. J Pediatr 144: 827–829.

Lane RJ, Dick JP, de Belleroche J. 1991. Glycine and neurodegenerative disease. Lancet 337:732–733.

Lane RJ, Virgo L, Lantos PL, de Belleroche J. 1998. A case of multiple system atrophy with hyperglycinaemia due to a selective deficiency of glycine transporter mRNA. Neuropathol Appl Neurobiol 24:353–358.

Leegwater PA, Vermeulen G, Konst AA, Naidu S, Mulders J, Visser A, Kersbergen P, Mobach D, Fonds D, van Berkel CG, Lemmers RJ, Frants RR, Oudejans CB, Schutgens RB, Pronk JC, van der Knaap MS. 2001. Subunits of the translation initiation factor eIF2B are mutant in leukoencephalopathy with vanishing white matter. Nat Genet 29:383–388.

Luder AS, Davidson A, Goodman SI, Greene CL. 1989. Transient nonketotic hyperglycinemia in neonates. J Pediatr 114: 1013–1015.

Mauillon JL, Michel P, Limacher JM, Latouche JB, Dechelotte P, Charbonnier F, Martin C, Moreau V, Metayer J, Paillot B, Frebourg T. 1996. Identification of novel germline hMLH1 mutations including a 22 kb Alu-mediated deletion in patients with familial colorectal cancer. Cancer Res 56:5728–5733.

Nakai T, Nakagawa N, Maoka N, Masui R, Kuramitsu S, Kamiya N. 2005. Structure of P-protein of the glycine cleavage system: implications for nonketotic hyperglycinemia. EMBO J 24: 1523–1536.

Nanao K, Okamura-Ikeda K, Motokawa Y, Danks DM, Baumgartner ER, Takada G, Hayasaka K. 1994a. Identification of the mutations in the T-protein gene causing typical and atypical nonketotic hyperglycinemia. Hum Genet 93:655–658.

Nanao K, Takada G, Takahashi E, Seki N, Komatsu Y, Okamura-Ikeda K, Motokawa Y, Hayasaka K. 1994b. Structure and chromosomal localization of the aminomethyltransferase gene (AMT). Genomics 19:27–30.

Ohya Y, Ochi N, Mizutani N, Hayakawa C, Watanabe K. 1991. Nonketotic hyperglycinemia: treatment with NMDA antagonist and consideration of neuropathogenesis. Pediatr Neurol 7: 65–68.

Okamura-Ikeda K, Ohmura Y, Fujiwara K, Motokawa Y. 1993. Cloning and nucleotide sequence of the gcv operon encoding the *Escherichia coli* glycine-cleavage system. Eur J Biochem 216: 539–548.

Pousi B, Hautala T, Heikkinen J, Pajunen L, Kivirikko KI, Myllyla R. 1994. Alu-Alu recombination results in a duplication of seven exons in the lysyl hydroxylase gene in a patient with the type VI variant of Ehlers-Danlos syndrome. Am J Hum Genet 55:899–906.

Sakata Y, Owada Y, Sato K, Kojima K, Hisanaga K, Shinka T, Suzuki Y, Aoki Y, Satoh J, Kondo H, Matsubara Y, Kure S. 2001. Structure and expression of the glycine cleavage system in rat central nervous system. Brain Res Mol Brain Res 94:119–130.

Schiffmann R, Kaye EM, Willis JK 3rd, Africk D, Ampola M. 1989. Transient neonatal hyperglycinemia. Ann Neurol 25: 201–203.

Sellner L, Edkins E, Greed L, Lewis B. 2005. Detection of mutations in the glycine decarboxylase gene in patients with nonketotic hyperglycinaemia. Mol Genet Metab 84:167–171.

Singer HS, Valle D, Hayasaka K, Tada K. 1989. Nonketotic hyperglycinemia: studies in an atypical variant. Neurology 39: 286–288.

Steiman GS, Yudkoff M, Berman PH, Blazer-Yost B, Segal S. 1979. Late-onset nonketotic hyperglycinemia and spinocerebellar degeneration. J Pediatr 94:907–911.

Stoppa-Lyonnet D, Duponchel C, Meo T, Laurent J, Carter PE, Arala-Chaves M, Cohen JH, Dewald G, Goetz J, Hauptmann G, Lagrue G, Lesavre P, Lopez-Trascasa M, Misiano G, Moraine C, Sobel A, Spöth PJ, Tosi M. 1991. Recombinational biases in the rearranged C1-inhibitor genes of hereditary angioedema patients. Am J Hum Genet 49:1055–1062.

Suzuki Y, Ueda H, Toribe Y. 2001. [Proton MR spectroscopy of nonketotic hyperglycinemia]. No To Hattatsu 33:422–425.

Tada K, Narisawa K, Yoshida T, Yokoyama K, Nakagawa H, Tanno K, Mochizuki K, Arakawa T, Yoshida T, Kikuchi G. 1969. Hyperglycinemia: a defect in glycine cleavage reaction. Tohoku J Exp Med 98:289–296.

Tada K, Hayasaka K. 1987. Non-ketotic hyperglycinaemia: clinical and biochemical aspects. Eur J Pediatr 146:221–227.

Takayanagi M, Kure S, Sakata Y, Kurihara Y, Ohya Y, Kajita M, Tada K, Matsubara Y, Narisawa K. 2000. Human glycine decarboxylase gene (GLDC) and its highly conserved processed pseudogene (psiGLDC): their structure and expression, and the identification of a large deletion in a family with nonketotic hyperglycinemia. Hum Genet 106:298–305.

Toone JR, Applegarth DA, Coulter-Mackie MB, James ER. 2000. Biochemical and molecular investigations of patients with nonketotic hyperglycinemia. Mol Genet Metab 70:116–121.

Toone JR, Applegarth DA, Coulter-Mackie MB, James ER. 2001. Recurrent mutations in P- and T-proteins of the glycine cleavage complex and a novel T-protein mutation (N145I): a strategy for the molecular investigation of patients with nonketotic hyperglycinemia (NKH). Mol Genet Metab 72:322–325.

Toone JR, Applegarth DA, Kure S, Coulter-Mackie MB, Sazegar P, Kojima K, Ichinohe A. 2002. Novel mutations in the P-protein (glycine decarboxylase) gene in patients with glycine encephalopathy (non-ketotic hyperglycinemia). Mol Genet Metab 76: 243–249.

Toone JR, Applegarth DA, Levy HL, Coulter-Mackie MB, Lee G. 2003. Molecular genetic and potential biochemical characteristics of patients with T-protein deficiency as a cause of glycine encephalopathy (NKH). Mol Genet Metab 79: 272–280.

Trauner DA, Page T, Greco C, Sweetman L, Kulovich S, Nyhan WL. 1981. Progressive neurodegenerative disorder in a patient with nonketotic hyperglycinemia. J Pediatr 98:272–275.

Turner SR, Ireland R, Rawsthorne S. 1992. Cloning and characterization of the P subunit of glycine decarboxylase from pea (*Pisum sativum*). J Biol Chem 267:5355–5360.

van der Knaap MS, Wevers RA, Kure S, Gabreels FJ, Verhoeven NM, van Raaij-Selten B, Jaeken J. 1999. Increased cerebrospinal fluid glycine: a biochemical marker for a leukoencephalopathy with vanishing white matter. J Child Neurol 14:728–731.

von Wendt L, Hirvasniemi A, Simila S. 1979. Nonketotic hyperglycinemia. A genetic study of 13 Finnish families. Clin Genet 15:411–417.

Wiltshire EJ, Poplawski NK, Harrison JR, Fletcher JM. 2000. Treatment of late-onset nonketotic hyperglycinaemia: effectiveness of imipramine and benzoate. J Inherit Metab Dis 23:15–21.

Zafra F, Aragon C, Gimenez C. 1997. Molecular biology of glycinergic neurotransmission. Mol Neurobiol 14:117–142.

Drug Metab. Pharmacokinet. 20 (4): *SNP21* (294)-*SNP26* (299) (2005).

SNP Communications

Two Novel Single Nucleotide Polymorphisms (SNPs) of the CYP2D6 Gene in Japanese Individuals

Aiko EBISAWA, Masahiro HIRATSUKA, Kanako SAKUYAMA, Yumiko KONNO, Takamitsu SASAKI and Michinao MIZUGAKI*

Department of Clinical Pharmaceutics, Tohoku Pharmaceutical University, Sendai, Japan

Full text of this paper is available at http://www.jstage.jst.go.jp/browse/dmpk

Summary: We analyzed all the exons and exon-intron junctions of the *CYP2D6* gene from 286 Japanese individuals. We detected two novel single nucleotide polymorphisms (SNPs) 2556C>T in exon 5 (Thr261Ile) and 3835A>C in exon 8 (Lys404Gln). Both these SNPs showed a frequency of 0.002.

Key words: CYP2D6; genetic polymorphism; Japanese

Introduction

CYP2D6 metabolizes more than 50 clinically important drugs including some tricyclic antidepressants, neuroleptics, and β-adrenergic blockers.[1] The *CYP2D6* gene locus is extremely polymorphic, with more than 80 allelic variants (http://www.imm.ki.se/CYPalleles/cyp2d6.htm). The homozygous of defective *CYP2D6* alleles, which result in the absence of CYP2D6 enzyme activity, are classified as poor metabolizer (PM) phenotypes. The frequency of PMs is 5%–10% in Caucasian population and less than 1% in Asian population.[1-6] Among the variant alleles reported to date, three alleles, *CYP2D6*3*, *CYP2D6*4*, and *CYP2D6*5*, have been reported to account for approximately 95% of the alleles of PMs in Caucasian population.[6,7] However, as yet, PMs associated with CYP2D6 function in the Japanese population could not be accounted for by the known variant alleles of *CYP2D6*.[8]

In the present study, we analyzed all the exons and exon-intron junctions of the *CYP2D6* gene from 286 Japanese individuals by using denaturing HPLC (DHPLC). Additionally, we identified two novel SNPs of the *CYP2D6* gene in Japanese individuals.

Materials and Methods

Venous blood was obtained from 286 unrelated healthy Japanese volunteers and patients admitted to Tohoku University Hospital. Written informed consent was obtained from all the blood donors, and the study was approved by the Local Ethics Committee of Tohoku University Hospital and Tohoku Pharmaceutical University. DNA was isolated from anticoagulated (with K_2EDTA) peripheral blood by using QIAamp DNA Mini Kits (Qiagen, Hilden, Germany) accordance with the manufacturer's instructions.

Long PCR was performed in order to amplify the entire *CYP2D6* gene and to detect the *CYP2D6*5* allele using primer pairs (**Table 1**), as described by Johansson *et al.*[9] Genomic DNA (10–50 ng) was amplified using LA-Taq DNA polymerase (TaKaRa Co., Kyoto, Japan). The amplification was performed on an iCycler (Bio-Rad, Hercules, CA, USA). The resultant PCR products were a 5-kb fragment contained the entire *CYP2D6* gene and a 6-kb fragment that indicated the presence of the *CYP2D6*5* allele. The thermal profile consisted of denaturation at 95°C for 5 minutes, followed by 30 cycles of denaturation at 95°C for

On March 1, 2005, these SNPs were not found in dbSNP in the National Center for Biotechnology Information (http://www.ncbi.nlm.nih.gov/SNP/), GeneSNPs at the Utah Genome Center (http://www.genome.utah.edu/genesnps/), or the Human CYP Allele Nomenclature Committee database (http://www.imm.ki.se/CYPalleles/). *CYP2D6*53* is consisted of two variants which have already found in dbSNP in the National Center for Biotechnology Information (http://www.ncbi.nlm.nih.gov/SNP/). However, this variant allele has not been registered found in the Human CYP Allele Nomenclature Committee database (http://www.imm.ki.se/CYPalleles/). The two *CYP2D6* haplotypes that possess each of 2556C>T (T261I) and 3835A>C (K404Q) were assigned as *CYP2D6*54* and *CYP2D6*55*, respectively, by the Human CYP Allele Nomenclature Committee (http://www.imm.ki.se/CYPalleles/).

Received; April 8, 2005, Accepted; May 19, 2005

**To whom correspondence should be addressed*: Michinao MIZUGAKI, Ph.D., *Department of Clinical Pharmaceutics, Tohoku Pharmaceutical University, 4-4-1, Komatsushima, Aoba-ku, Sendai 981-8558, Japan. Tel. +81-22-234-4181, Fax. +81-22-275-2013, E-mail: mizugaki@tohoku-pharm.ac.jp*

Table 1. Primers used for the amplification of the entire *CYP2D6* gene and identification of the *CYP2D6*5* allele

	5′ Primer	3′ Primer	Annealing Temp. (°C)
entire *CYP2D6* gene	ccagaaggctttgcaggcttca	actgagccctgggaggtaggta	65.0
*CYP2D6*5* allele	gccactctcgtgtcgtcagcttt	ggcatgagctaaggcacc	61.2

Table 2. Amplification and DHPLC conditions for *CYP2D6* SNP analysis of genomic DNA

Exon	Size (bp)	5′ Primer	3′ Primer	Predicted Temp. (°C)	DHPLC Temp. (°C)
1	280	gtgggggtgccaggtgtgtccagaggagcc	ggtaggggagcctcagcacctctgccgccc	63.4	63.4, 66.0
2	272	agtctggggtgatcctggcttgacaagagg	cacccacccgggtcccacggaaatctgtct	64.7	64.7, 67.0
3	253	gtggggctaatgccttcatggccacgcgca	gtcccccgccttcccagttcccgctttgtg	65.4	65.4
4	261	aaggcgggggacggggaaggcgacccctta	acctctcgggagctcgccctgcagagactc	65.4	64.4
5	277	ggtgaacgcagagcacaggagggattgaga	gggacgctcaacccaccaccctttgcccccc	63.2	62.2
6	242	atttgggggctaccccgttctgtcccgagt	cctgtacccttcctccctcggcccctgcac	63.6	62.6
7	287	gccggacccccctgggtgctgacccattgtg	tatcaccaggtgctggtgctgagctggggt	63.6	62.6
8	242	ccagcatcctagagtccagtccccactctc	cctgcaagactccacggaaggggacaggga	63.4	63.4
9	277	ggggtatcacccaggagccaggctcactga	cattagagcctctggctagggagcaggctg	63.0	63.0

1 minute, annealing for 1 minute, extension at 68°C for 5 minutes, and a final extension at 72°C for 7 minutes. The annealing temperatures for long PCR summarized in **Table 1**.

All the *CYP2D6* specific products, diluted 1:10 in water, were used as a DNA template for a second round PCR of all the *CYP2D6* exons. **Table 2** lists the primer pairs that were used to amplify *CYP2D6* exons. These primers were designed based on the genomic sequence reported in GenBank (M33388). Amplicons were generated with the AmpliTaq Gold PCR Master Mix (Applied Biosystems, Foster City, CA, USA). The thermal profile consisted of denaturation at 95°C for 10 minutes, followed by 30 cycles of denaturation at 95°C for 30 seconds, annealing at 60°C for 30 seconds, extension at 72°C for 30 seconds, and a final extension at 72°C for 7 minutes. Heteroduplexes were generated by thermal cycling as follows: 95°C for 1 minute, followed by a reduction in temperature from 95°C by 45 increments of 1.5°C per minute.

The PCR products were analyzed using the DHPLC system, WAVE® (Transgenomic Inc., Omaha, NE, USA). Unpurified PCR samples (5 μL) were separated on a heated C18 reverse phase column (DNASep®) using 0.1 M triethylammonium acetate (TEAA) in water and 0.1 M TEAA in 25% acetonitrile at a flow rate of 0.9 mL/min. The software provided with the instrument selected the temperature for the heteroduplex separation in the heterozygous CYP2D6 fragment. **Table 2** summarizes the DHPLC running conditions for each amplicon. The linear acetonitrile gradient was adjusted to the retention time of the DNA peak at 4–5 minutes. Homozygous nucleotide exchanges can sometimes be distinguished due to a slight shift in the elution time when compared with the reference. The addition of an approximately equal amount of wild-type DNA to the samples (1:1) prior to the denaturation step enabled homozygous alterations to be detected reliably. This was done routinely for all the samples in order to identify homozygous sequence variations. Therefore, all the samples were first analyzed without mixing with an equal amount of wild-type DNA; subsequently, wild-type DNA was mixed with each sample to detect homozygous variants. The resultant chromatograms were compared with the chromatograms of wild-type DNA.

Both strands of samples with variants detected using DHPLC were analyzed using a CEQ8000® automated DNA sequencer (Beckman-Coulter Inc., Fullerton, CA, USA). We also sequenced all the samples with chromatographic findings that differed from the wild-type DNA in order to establish links between mutations and specific profiles. We sequenced the PCR products by the fluorescent dideoxy termination sequencing using the DTCS DNA Sequencing Kit (Beckman-Coulter Inc.) accordance with the manufacturer's instructions.

For the haplotype analysis of *CYP2D6* variant alleles, the PCR products of entire *CYP2D6* genes were

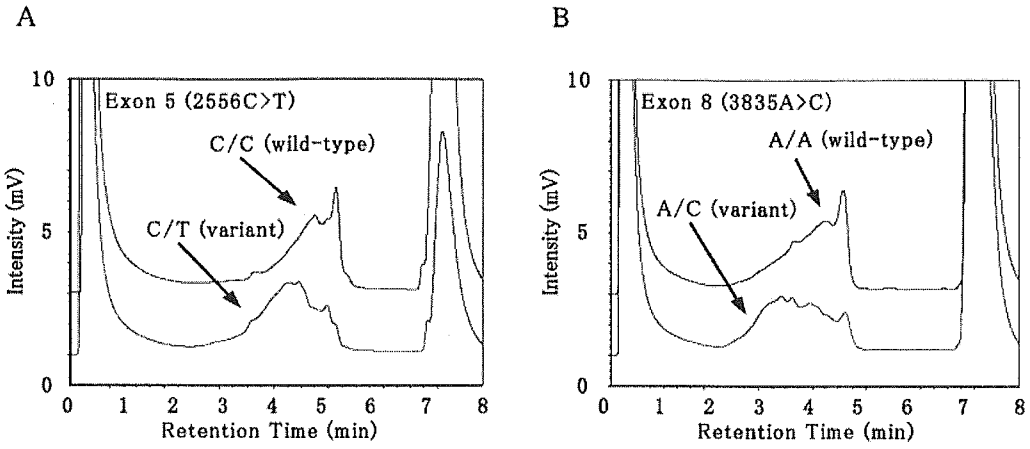

Fig. 1. DHPLC chromatograms of exon 5 (A) and exon 8 (B) of human *CYP2D6* gene. The elution profiles of heterozygous sequence variants are compared with a reference wild-type DNA chromatogram.

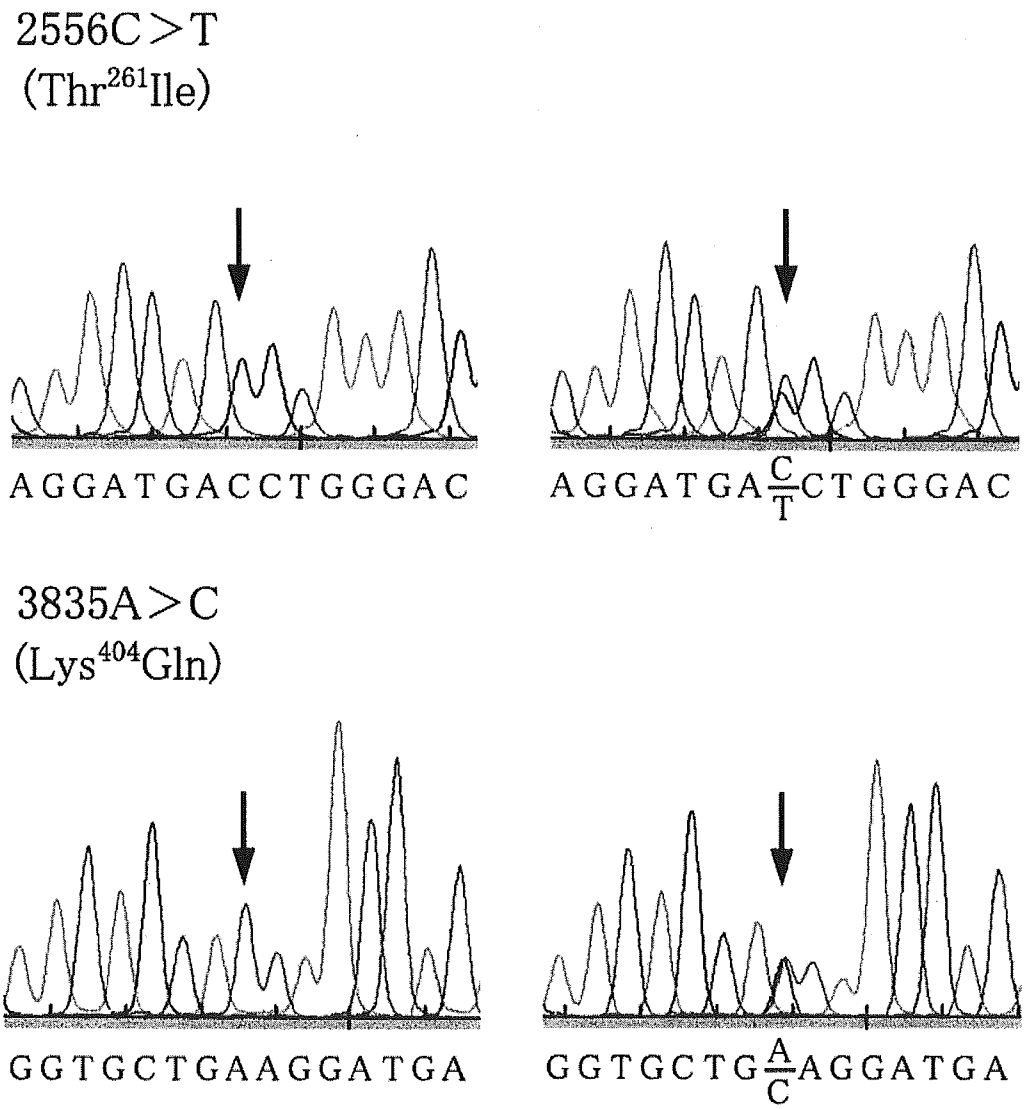

Fig. 2. The nucleotide sequences of the *CYP2D6* gene in exon 5 and exon 8. Although sequences are shown for sense strands, both strands were sequenced. Arrows indicate the variant nucleotide positions.

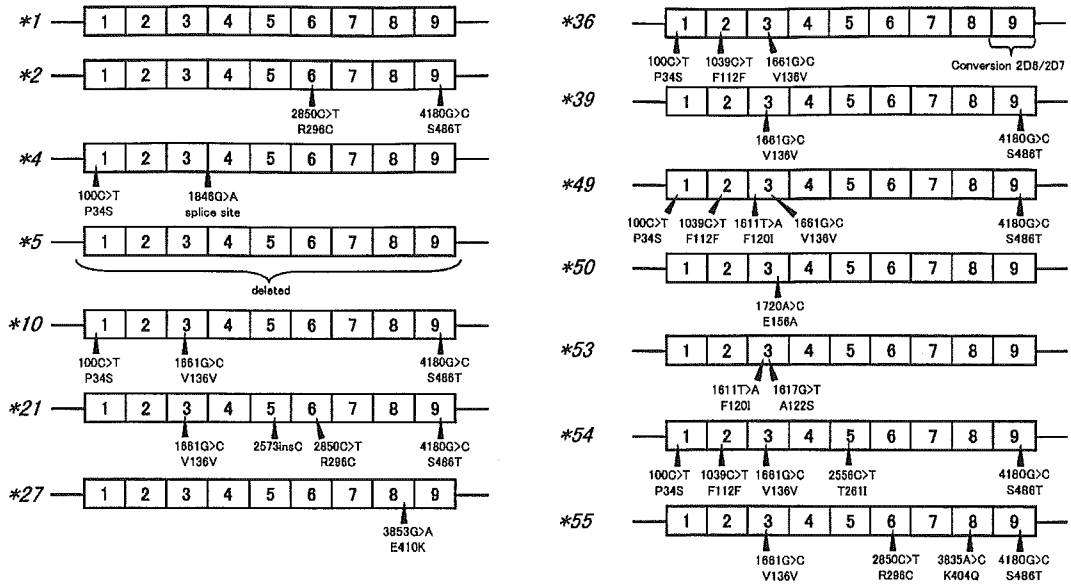

Fig. 3. Structure of *CYP2D6* alleles isolated from the Japanese individuals. The 9 exons of *CYP2D6* are indicated by numbered boxes. The positions of the various polymorphisms associated with each allele are indicated.

subcloned into a pCR®-XL-TOPO® vector (Invitrogen Co., CA, USA). The clones inserted into the CYP2D6 fragments were sequenced using a CEQ8000® automated DNA sequencer.

Results and Discussion

We found two novel SNPs as follows:
1) SNP: 050301Hiratsuka04; GENE-NAME: *CYP2D6*; ACCESSION NUMBER: M33388; LENGTH: 25 bases; 5′-AGCACAGGATGAC/TCTGGGACCCAGC-3′.
2) SNP: 050301Hiratsuka05; GENE-NAME: *CYP2D6*; ACCESSION NUMBER: M33388; LENGTH: 25 bases; 5′-TCATCGGTGCTGA/CAGGATGAGGCCG-3′.

The DHPLC chromatograms and the electrophoretograms of the novel SNPs are shown in **Figs. 1 and 2**, respectively. The first SNP was 2556C>T in exon 5 resulting in an amino acid change of Thr261Ile. Haplotype analysis indicated that 100C>T, 1039C>T, 1661G>C, and 4180G>C existed in the same allele of the *CYP2D6* gene (**Fig. 3**). Of the 286 individuals, one was heterozygous for the 2556C>T SNP, suggesting that the allele frequency was 0.002 in the Japanese population. The second SNP was 3835A>C in exon 8 resulting in an amino acid change of Lys404Gln. Haplotype analysis indicated that 1661G>C, 2850C>T, and 4180G>C existed in the same allele of the *CYP2D6* gene (**Fig. 3**). Of the 286 individuals, one was heterozygous for the 3835A>C SNP, suggesting that the allele frequency was 0.002 in the Japanese population. The sequences for each sample were obtained from at least two different PCR amplifications.

These novel SNPs are located in the exons of the *CYP2D6* gene and result in amino acid substitutions. The Thr261 and Lys404 in CYP2D6 are located in G-helix and K″-helix, respectively.[10-12] These amino acid residues are not mapped in substrate recognition sited, but are conserved in the CYP2D subfamily in mammals.[13] Thus, these amino acid substitutions, Thr261Ile and Lys404Gln, are expected to alter the catalytic properties of the CYP2D6. Further studies are required to elucidate the functional characteristics of these novel variant alleles of the *CYP2D6* gene.

In the present study, fourteen *CYP2D6* alleles were detected in all the 286 Japanese individuals. The most frequent variant allele was *CYP2D6*10*, followed by **2*, **5*, and **21*, and their frequencies were observed to be 0.362, 0.112, 0.072, and 0.007, respectively. The most frequent defective allele in the Japanese population is *CYP2D6*5*, which is associated with the PM phenotype. To date, the non-functional alleles of *CYP2D6* that have been observed in Japanese population are *CYP2D6*4*, **5*, **14*, **18*, **21*, and **44*. However, none of the 286 individuals analyzed at least by DHPLC method in this study showed the presence of *CYP2D6*14*, **18*, or **44*. This discrepancy may be caused by differences in sample sizes among these studies. Soyama *et al.*[14] have recently reported the detection of five novel alleles, *CYP2D6*47*, **48*, **49*, **50*, and **51*. In the present study, *CYP2D6*49* and **50* alleles were also found, with frequencies of 0.003 and 0.002, respectively.

The 23 different genotypes found in this study are listed together with their respective frequencies in **Table 3**. The most frequent genotypes were *CYP2D6*1/*10*, **1/*